

Evolution of unpolarized transverse momentum dependent parton distributions of twist-3

Xue-Tao Liu,¹ Ping-An Liu,¹ Yu-Lu Liu,¹ and An-Ping Chen^{1,2,*}

¹*College of Physics and Communication Electronics,
Jiangxi Normal University, Nanchang 330022, China*

²*Jiangxi Provincial Key Laboratory of Advanced Electronic
Materials and Devices, Nanchang 330022, China*

Abstract

We revisit the calculation of the evolution equations for four unpolarized twist-3 transverse momentum dependent (TMD) parton distribution functions (PDFs) at $\mathcal{O}(\alpha_s)$. Unlike the existing calculations in the literature, which are based on the background field method, we derive the evolution equations directly through diagram expansion. Additionally, instead of using the δ regulator, we employ the exponential regulator to regularize the rapidity divergences. We find that the evolutions of the four twist-3 TMD PDFs are governed by eight homogeneous equations. Our evolution kernels agree with one set of results in the literature, but differ from another by a sign. Considering the advantages of the exponential regulator in high-order perturbative calculations, our results are crucial for computing the twist-3 TMD PDFs at $\mathcal{O}(\alpha_s^2)$.

* chenanning@jxnu.edu.cn

I. INTRODUCTION

The Transverse-Momentum-Dependent (TMD) distributions, such as TMD Parton Distribution Functions (TMD PDFs) and TMD Fragmentation Functions (TMD FFs), are non-perturbative and universal quantities that arise from TMD factorization theorems [1, 2]. These distributions play a critical role in determining the three-dimensional structure of hadrons. At the twist-2 or leading power (LP) level, TMD factorization has been established for several processes, such as Semi-Inclusive Deeply Inelastic Scattering (SIDIS) [1, 3], Drell-Yan processes [2, 4] and e^+e^- collisions [5]. The twist-2 TMD distributions have been extensively studied. It is well-known that twist-2 TMD distributions suffer from both ultraviolet (UV) divergences and rapidity divergences if they are defined with light-cone gauge links. The UV divergences can be regulated by using dimensional regularization with $d = 4 - 2\epsilon$ dimensions, which give rise to the renormalization scale μ . However, rapidity divergences are not regularized by dimensional regularization, and a dedicated regulator is required, generically denoted as τ . This introduces the rapidity scale ν dependence in TMD distributions.

In the literature, various rapidity regulators have been proposed to regularize the rapidity divergences. In Refs. [1, 2, 6], the gauge links off light-cone are employed in the definition of TMD distributions. In [5] a subtraction method is used to regulate the rapidity divergences, in which the gauge links in the TMD distributions are along light-cone directions, and the rapidity divergences are subtracted by a soft factor, which is defined with gauge links along light-cone directions and those off light-cone. In [7–10] variations of the analytic regulator were used. In [11–13], the δ regulator was used, in which finite imaginary parts in certain propagators were used to regulate the rapidity divergences. And in [14] the so-called exponential regulator was proposed. For more details about these different rapidity regulators, please refer to Refs. [15, 16]. Using analytic regulator, δ regulator and exponential regulator, the quark and gluon TMD PDFs and FFs have been perturbatively calculated at next-to-next-to-leading order (NNLO) [17–21]. Especially, using exponential regulator, the calculations of quark and gluon TMD PDFs and FFs have been carried out at next-to-next-to-next-to-leading order (N³LO) [22–25]. On the other hand, the presence of scales μ and ν leads to two evolution equations for twist-2 TMD distributions: the renormalization group (RG) evolution equations and rapidity scale evolution equations—the Collins-Soper

(CS) equations. The evolution kernels of both evolution equations have been calculated up to NNLO [26–28].

Compared to twist-2 TMD factorization, research on twist-3 or next-to-leading power (NLP) TMD factorization is much less developed. In the early works of [29–32], a comprehensive tree-level factorization formalism for the SIDIS process, expressed in terms of both twist-2 and twist-3 TMD distributions, was established. This tree-level methodology was further applied to e^+e^- annihilation in [33] and Drell-Yan process in [34]. Early studies beyond tree-level were carried out in Refs. [35–37]. In [35, 37] the authors considered the matching between the TMD and collinear descriptions in the intermediate transverse momentum region at the twist-3 level. In [36] the authors performed a calculation of the unpolarized twist-3 TMD PDF at NLO ($\mathcal{O}(\alpha_s)$) and derived the Collins-Soper equation for it. In their study the rapidity divergences were regularized by using off-light-cone gauge links. In recent years, a complete expression for twist-3 TMD factorization beyond the tree level has been derived by different groups using various methods. These include the background field method [38], the Soft-Collinear Effective Theory (SCET) [39], and the Collins-Soper-Sterman (CSS) factorization formalisms [40]. Furthermore, using the background field method, the authors studied the RG evolution equations and the Collins-Soper equations of TMD distributions at twist-3 in Refs. [38, 41, 42], where the RG evolution equations are discussed for the first time. In their studies, the δ regulator is used to regularize the rapidity divergences. However, there is a sign difference between the RG evolution kernels in [41] and those in [42]. Therefore, an independent calculation of the evolution equations is essential.

In this paper, we revisit the calculation of the RG evolution equations and the Collins-Soper equations for twist-3 TMD PDFs at $\mathcal{O}(\alpha_s)$. We consider the unpolarized twist-3 quark-gluon-quark correlators in this work. Compared to the calculations in Refs. [38, 41, 42], we derive the evolution equations straightforwardly by the diagram expansion. On the other hand, in our calculation we employ the exponential regulator to regularize the rapidity divergences. Compared to other regulators, one of the advantages of the exponential regulator is that it is applied to the total momentum of the extra emissions in the final state. Aside from this last integration, the regulator does not alter the structure of the (cut)-propagators in the amplitudes. Because of this, one can employ many modern techniques, such as integration-by-parts (IBP) method and differential equations, to perform the loop

integration [20]. This allows one to derive the twist-2 TMD PDFs and FFs at high orders, as showed in [20–25]. And this method can also be extended to the NNLO calculation of the twist-3 TMD PDFs. However, before proceeding with such calculations, it is necessary to first derive the RG evolution equations for these distributions.

The rest of the paper is organized as following. In section II we give the definition and parameterization of the unpolarized twist-3 quark-gluon-quark correlation function. In section III we use the equation of motion to separate the contributions from quark-quark correlation function at different twists. In section IV we give the details to calculate the RG evolution equations and the Collins-Soper equations for twist-3 TMD PDFs at $\mathcal{O}(\alpha_s)$. We perform the soft subtraction for twist-3 TMD PDFs and deriving the evolution equations for the subtracted TMD PDFs in section V, and section VI contains our summary. Finally, we list the evolution equations in different support domains in appendix A.

II. DEFINITION AND PARAMETERIZATION

In this work we use the light-cone coordinate system. In this system a vector a^μ is expressed as $a^\mu = (a^+, a^-, a_\perp) = ((a^0 + a^3)/\sqrt{2}, (a^0 - a^3)/\sqrt{2}, a^1, a^2)$ and $a_\perp^2 = -(a^1)^2 - (a^2)^2$. We introduce two light-like vectors $n^\mu = (0, 1, 0, 0)$ and $l^\mu = (1, 0, 0, 0)$. Using them we further define two transverse tensors $g_\perp^{\mu\nu} = g^{\mu\nu} - n^\mu l^\nu - n^\nu l^\mu$ and $\epsilon_\perp^{\mu\nu} = \epsilon^{\alpha\beta\mu\nu} l_\alpha n_\beta$. The transverse part of any vector a^μ can then be obtained as $a_\perp^\mu = g_\perp^{\mu\nu} a_\nu$. We further define $a_T^2 = -a_\perp^2$.

We consider the unpolarized twist-3 quark-gluon-quark distribution correlation function, whose definition is given by [40]

$$\begin{aligned} \Phi_F^\mu(x_1, x_2, k_{3\perp}) = & ig_s \int \frac{d\eta}{2\pi} \frac{d^3\xi}{(2\pi)^3} e^{-i\xi \cdot k_3 + i\eta n \cdot k_2} \\ & \times \langle h_A | \bar{\psi}(\xi) \mathcal{L}_n^\dagger(\xi) \mathcal{L}_n(\eta n) G^{+\mu}(\eta n) \mathcal{L}_n^\dagger(\eta n) \mathcal{L}_n(0) \psi(0) | h_A \rangle \Big|_{\xi^+ = 0}, \end{aligned} \quad (1)$$

here h_A is a unpolarized hadron with momentum $P_A^\mu = (P_A^+, 0, 0, 0)$, ψ is the quark field, $G^{+\mu}$ is the gluon field-strength tensor, \mathcal{L}_n is the gauge link along the direction n^μ

$$\mathcal{L}_n(\xi) = P \exp \left(-ig_s \int_0^\infty d\lambda n \cdot A(\lambda n + \xi) \right). \quad (2)$$

The sign convention for the strong coupling is $D^\mu = \partial^\mu + ig_s A^\mu$. Here we have neglected the transverse gauge links [43, 44], as in Feynman gauge the gluon field strength vanishes

at infinity. However, the transverse gauge links are important in certain singular gauges, like the light-cone gauge [43–46]. In above definition, k_3 is the momentum of the quark that is isolated on one side of the cut, x_1 is the momentum fraction associate with the other quark: $k_1^+ = x_1 P_A^+$, and x_2 denotes the momentum fraction of the gluon: $k_2^+ = x_2 P_A^+$. These momentum satisfy $k_3 = k_2 + k_1$, and we denote $k_3^+ = x_3 P_A^+$.

The parametrization for the correlation function (1) is given in Refs. [32, 39–41], which reads

$$\begin{aligned} & \Phi_F^\mu(x_1, x_2, k_{3\perp}) \\ &= \frac{x_3 M_A}{2} \left[(f^\perp - i g^\perp) \frac{k_{3\perp\nu}}{M_A} (g_\perp^{\mu\nu} - i \epsilon_\perp^{\mu\nu} \gamma_5) \frac{\gamma^-}{2} + (f^\perp + i g^\perp) \frac{k_{3\perp\nu}}{M_A} (g_\perp^{\mu\nu} + i \epsilon_\perp^{\mu\nu} \gamma_5) \frac{\gamma^-}{2} \right. \\ & \quad \left. + i h \frac{\gamma_\perp^\mu \gamma^-}{2} + i h^\perp \frac{\gamma_{\perp\nu} \gamma^-}{2} \left(2 g_\perp^{\nu\rho} g_\perp^{\mu\sigma} - g_\perp^{\nu\mu} g_\perp^{\rho\sigma} \right) \frac{k_{3\perp\rho} k_{3\perp\sigma}}{M_A^2} \right]. \end{aligned} \quad (3)$$

The twist-3 TMD PDFs on the r.h.s. depend on x_1 , x_2 and k_{3T}^2 . In above parametrization M_A is the mass of hadron h_A . In general the distribution functions f^\perp , g^\perp , h and h^\perp are complex. We define the corresponding distributions in b -space by following Fourier transforming,

$$\tilde{\Phi}_F^\mu(x_1, x_2, b_\perp) = \int d^2 k_{3\perp} e^{i k_{3\perp} \cdot b_\perp} \Phi_F^\mu(x_1, x_2, k_{3\perp}). \quad (4)$$

Using [39]

$$\int d^2 k_\perp e^{i k_\perp \cdot b_\perp} \frac{k_\perp^\mu}{M_A} f(k_\perp^2) = -i M_A b_\perp^\mu \tilde{f}^{(1)}(b_\perp^2), \quad (5a)$$

$$\int d^2 k_\perp e^{i k_\perp \cdot b_\perp} \frac{k_\perp^\mu k_\perp^\nu}{M_A^2} f(k_\perp^2) = \frac{(-i)^2}{2} M_A^2 b_\perp^\mu b_\perp^\nu \tilde{f}^{(2)}(b_\perp^2) + (-i)^2 g_\perp^{\mu\nu} \tilde{f}^{(1)}(b_\perp^2), \quad (5b)$$

we then obtain the parametrization in b -space as

$$\begin{aligned} & \tilde{\Phi}_F^\mu(x_1, x_2, b_\perp) \\ &= \frac{x_3 M_A}{2} \left[(\tilde{f}^{\perp(1)} - i \tilde{g}^{\perp(1)}) (-i M_A b_{\perp\nu}) (g_\perp^{\mu\nu} - i \epsilon_\perp^{\mu\nu} \gamma_5) \frac{\gamma^-}{2} + (\tilde{f}^{\perp(1)} + i \tilde{g}^{\perp(1)}) (-i M_A b_{\perp\nu}) \right. \\ & \quad \times (g_\perp^{\mu\nu} + i \epsilon_\perp^{\mu\nu} \gamma_5) \frac{\gamma^-}{2} + i \tilde{h} \frac{\gamma_\perp^\mu \gamma^-}{2} + i \tilde{h}^{\perp(2)} \frac{\gamma_{\perp\nu} \gamma^-}{2} \left(2 g_\perp^{\nu\rho} g_\perp^{\mu\sigma} - g_\perp^{\nu\mu} g_\perp^{\rho\sigma} \right) \\ & \quad \left. \times \frac{(-i)^2}{2} M_A^2 b_{\perp\rho} b_{\perp\sigma} \right]. \end{aligned} \quad (6)$$

Following Refs. [39, 47], here we defined the derivative of the TMD PDFs as

$$\tilde{f}^{(n)}(x_1, x_2, b_\perp) = n! \left(- \frac{2}{M_A^2} \frac{\partial}{\partial b_T^2} \right)^n \tilde{f}(x_1, x_2, b_\perp). \quad (7)$$

Based on above parametrization, the relevant traces of the quark-gluon-quark correlator are given by

$$\frac{1}{2x_3} \text{Tr}[\Phi_{F\nu}(x_1, x_2, k_{3\perp})(g_{\perp}^{\mu\nu} + i\epsilon_{\perp}^{\mu\nu} \gamma_5) \gamma^+] = k_{3\perp}^{\mu}(f^{\perp} - ig^{\perp}), \quad (8a)$$

$$\frac{1}{2x_3} \text{Tr}[\Phi_{F\nu}(x_1, x_2, k_{3\perp})(g_{\perp}^{\mu\nu} - i\epsilon_{\perp}^{\mu\nu} \gamma_5) \gamma^+] = k_{3\perp}^{\mu}(f^{\perp} + ig^{\perp}), \quad (8b)$$

$$\frac{1}{(d-2)x_3 M_A} \text{Tr}[\Phi_{F\nu}(x_1, x_2, k_{3\perp})(i\gamma_{\perp}^{\nu} \gamma^+)] = h, \quad (8c)$$

$$\begin{aligned} & \frac{M_A}{(d-2)x_3} \text{Tr}[\Phi_{F\mu}(x_1, x_2, k_{3\perp})(i\gamma_{\perp\mu} \gamma^+)] \left((d-2)g_{\perp}^{\nu\rho} g_{\perp}^{\mu\sigma} - g_{\perp}^{\nu\mu} g_{\perp}^{\rho\sigma} \right) \\ &= \left((d-2)g_{\perp}^{\nu'\rho} g_{\perp}^{\mu'\sigma} - g_{\perp}^{\nu'\mu'} g_{\perp}^{\rho\sigma} \right) k_{3\perp\nu'} k_{3\perp\mu'} h^{\perp}. \end{aligned} \quad (8d)$$

Here $d = 4 - 2\epsilon$ is the space-time dimension. These TMD PDFs depend not only on momentum fractions, but also on the renormalization scale μ and rapidity scale ν implicitly. The μ and ν -dependence for the TMD PDFs in Eq.(8) is the subject of this work. It should be noted that the TMD PDFs of twist-3 are indefinite at $x_i = 0$, ($i = 1, 2, 3$) as demonstrated in [41]. Nonetheless, they are integrable at $x_i = 0$ [41]. For simplicity, in following derivation we assume $x_i > 0$. The evolution equations in other support domains can be calculated similarly, and we present them in the appendix. In our following calculation of the evolution equations we will use the Feynman gauge.

III. EQUATION OF MOTION RELATIONS

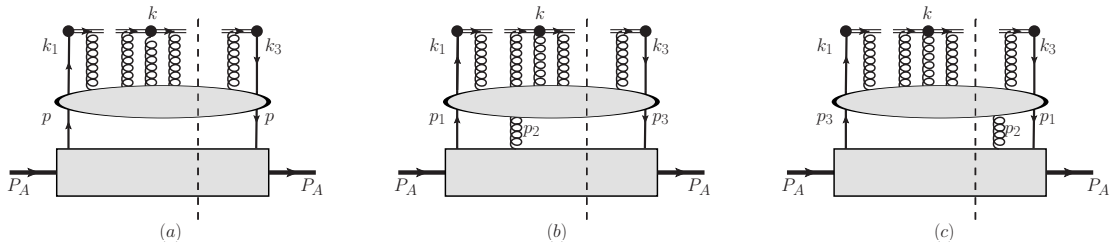


FIG. 1. The generic structure of diagrams for evolutions.

In order to derive the evolution equations of the twist-3 TMD PDFs, we essentially need to consider the contribution of Fig.1. Fig.1(a), Fig.1(b) and Fig.1(c) stand for the generic structure of diagrams for the contributions from quark-quark correlation function and quark-gluon-quark correlation function, respectively. In the diagrams the black solid circles stand

for the insertion of the field operators with given projections of γ -matrices in the definitions of twist-3 TMD PDFs in Eq.(8). The double line represent the gauge link. The middle bubbles represent various parton scatterings. The boxes in the lower part of the diagrams in Fig.1(b) and Fig.1(c) denote the quark-gluon-quark correlation function and its hermitian conjugate, respectively. And that in Fig.1(a) denotes the quark-quark correlation function. The quark-quark correlation function is defined as

$$\Phi(x, p_\perp) = \int \frac{d^3\xi}{(2\pi)^3} e^{-i\xi \cdot p} \langle h_A | \bar{\psi}(\xi) \mathcal{L}_n^\dagger(\xi) \mathcal{L}_n(0) \psi(0) | h_A \rangle \Big|_{\xi^+=0}, \quad (9)$$

here p is the momentum carried by the quark, x is the corresponding momentum fraction: $p^+ = xP_A^+$. It should be noted that the quark-quark correlation function contains the contributions at different twists. Following the discussion in Refs. [40, 48], to separate the contributions at different twists, we decompose the quark field ψ into the good and bad components:

$$\psi(\xi) = \psi_+(\xi) + \psi_-(\xi), \quad \psi_+(\xi) = \frac{1}{2} \gamma^- \gamma^+ \psi(\xi), \quad \psi_-(\xi) = \frac{1}{2} \gamma^+ \gamma^- \psi(\xi), \quad (10)$$

here ψ_+ is the good component, which is not power suppressed, while ψ_- is the bad component and it is power suppressed compared to ψ_+ . Inserting the decomposition Eq.(10) into Eq.(9), we separate the contributions at twist-2 and twist-3. The twist-2 quark-quark correlation function, which contain only good components, is given by

$$\Phi^{\text{LP}}(x, p_\perp) = \int \frac{d^3\xi}{(2\pi)^3} e^{-i\xi \cdot p} \langle h_A | \bar{\psi}_+(\xi) \mathcal{L}_n^\dagger(\xi) \mathcal{L}_n(0) \psi_+(0) | h_A \rangle \Big|_{\xi^+=0}. \quad (11)$$

Its parameterization is well-known [32, 39–41]

$$\frac{1}{2} \text{Tr}[\Phi^{\text{LP}}(x, p_\perp) \gamma^+] = f_1(x, p_\perp), \quad (12a)$$

$$\frac{1}{2} \text{Tr}[\Phi^{\text{LP}}(x, p_\perp) (i\sigma^{\alpha+} \gamma^5)] = - \frac{\epsilon_\perp^{\alpha\rho} p_{\perp\rho}}{M_A} h_1^\perp(x, p_\perp). \quad (12b)$$

The correlation functions which contain one good field and one bad field are power suppressed compared to Φ^{LP} . We refer to their sum as twist-3 quark-quark correlation function, which is given by

$$\begin{aligned} \Phi^{\text{NLP}}(x, p_\perp) &= \Phi^{\text{NLP},A}(x, p_\perp) + \Phi^{\text{NLP},B}(x, p_\perp), \\ \Phi^{\text{NLP},A}(x, p_\perp) &= \int \frac{d^3\xi}{(2\pi)^3} e^{-i\xi \cdot p} \langle h_A | \bar{\psi}_+(\xi) \mathcal{L}_n^\dagger(\xi) \mathcal{L}_n(0) \psi_-(0) | h_A \rangle \Big|_{\xi^+=0}, \end{aligned}$$

$$\Phi^{\text{NLP},B}(x, p_\perp) = \int \frac{d^3\xi}{(2\pi)^3} e^{-i\xi \cdot p} \langle h_A | \bar{\psi}_-(\xi) \mathcal{L}_n^\dagger(\xi) \mathcal{L}_n(0) \psi_+(0) | h_A \rangle \Big|_{\xi^+=0}. \quad (13)$$

Finally, the correlation function that contain only bad components is twist-4 correlation function, it is irrelevant for our study.

Using the equation of motion: $2D^+\psi_- + \gamma^+\gamma_\perp \cdot D_\perp \psi_+ = 0$ [32, 40], one can express the bad field in the correlation functions in Eq.(13) with the good field combined with gluon fields. Take $\Phi^{\text{NLP},A}$ as a example, we have [40, 48]

$$\begin{aligned} & \Phi^{\text{NLP},A}(x, p_\perp) \\ &= \int \frac{d^3\xi}{(2\pi)^3} e^{-i\xi \cdot p} \langle h_A | \bar{\psi}_+(\xi) \mathcal{L}_n^\dagger(\xi) \mathcal{L}_n(0) \frac{i\gamma^+}{2p^+} (i\gamma_\perp \cdot p_\perp) \psi_+(0) | h_A \rangle \Big|_{\xi^+=0} \\ &+ \int dp_2^+ \frac{i}{p_2^+} \int \frac{d\eta}{2\pi} \frac{d^3\xi}{(2\pi)^3} e^{-i\xi \cdot p + i\eta n \cdot p_2} \\ &\times \langle h_A | \bar{\psi}_+(\xi) \mathcal{L}_n^\dagger(\xi) \mathcal{L}_n(\eta n) G^{a,+ \mu}(\eta n) \mathcal{L}_n^\dagger(\eta n) \mathcal{L}_n(0) \frac{i\gamma^+}{2p^+} (-ig_s \gamma_\mu T^a) \psi_+(0) | h_A \rangle \Big|_{\xi^+=0}. \end{aligned} \quad (14)$$

We find the first term on the r.h.s. is the twist-2 quark-quark correlation function Φ^{LP} , but contains power correction associated with p_\perp . And the second term is the twist-3 quark-gluon-quark correlation function.

Using the relations in Eqs. (11), (13) and (14), we are now able to correctly separate contributions at different twists from Fig.1(a). The contribution from twist-2 correlation functions can be obtained by calculating Fig.1(a) with the bottom-box replaced by the Φ^{LP} , as showed in Fig.2(a), where the bottom-box represents Φ^{LP} . The contribution from twist-3 correlation functions can be obtained by replacing the bottom-box in Fig.1(a) with the terms on the r.h.s. of Eq. (14), as showed in Fig.2(b-e). Fig.2(b) stands for the contribution from the term in the second line of Eq. (14), where the bottom-box represents Φ^{LP} , the quark line with the short bar represents the special propagator $i\gamma^+/2p^+$, and the black dot near the bottom-box denotes the vertex $i\gamma_\perp \cdot p_\perp$. Fig.2(c) is the contribution from the hermitian conjugate. Fig.2(d) and (e) stand for the contributions from the term in the last line of Eq. (14), where the bottom-boxes represent the twist-3 quark-gluon-quark correlation function and its hermitian conjugate, respectively.

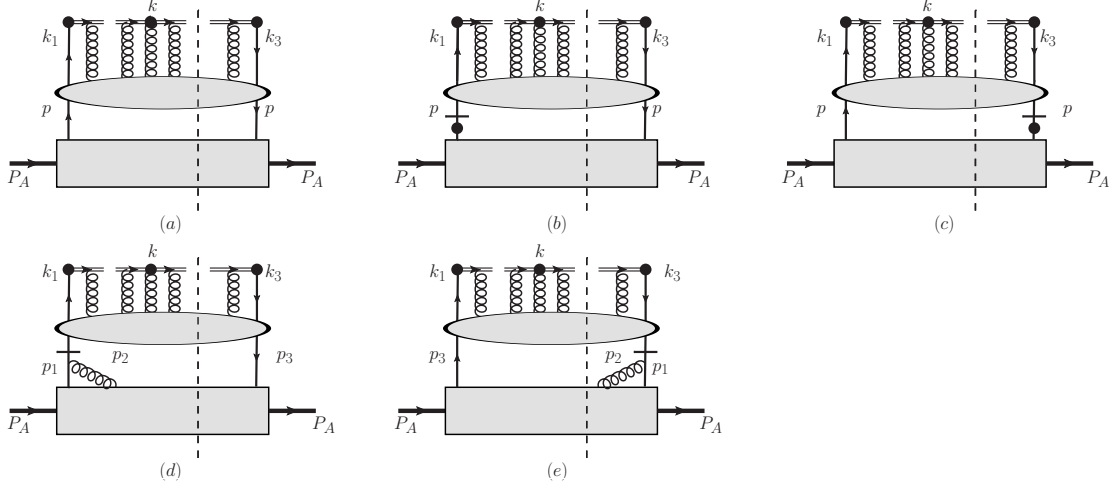


FIG. 2. Patterns of diagrams representing contributions from the quark-quark correlation function after applying the equation of motion.

IV. EVOLUTION EQUATIONS

With the above discussion, we are now able to calculate the evolution equations of the twist-3 TMD PDFs based on the diagrams in Fig.1(b), Fig.1(c) and Fig.2(a-e). In the calculation, we employ the $\overline{\text{MS}}$ scheme to subtract the UV divergences. Consequently, there is a factor $[\mu^2 \exp(\gamma_E)/(4\pi)]^\epsilon$ associated with each factor of the strong coupling $\alpha_s = g_s^2/(4\pi)$.

We take the distribution function h as a example to show the calculation. The contributions from twist-2 quark-quark correlation function at LO ($\mathcal{O}(\alpha_s)$) are showed in Fig.3. Here

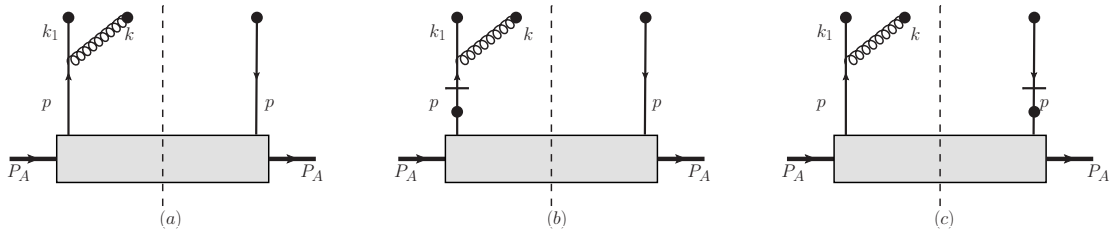


FIG. 3. Diagrams for the contributions from twist-2 quark-quark correlation function.

the real diagrams have no contribution because they have no UV or rapidity divergences. From Fig.3(a) we have

$$h(x_1, x_2, k_{3\perp}) \Big|_{3a} = \frac{ig_s}{(d-2)x_3 M_A} \left(\frac{\mu^2 e^{\gamma_E}}{4\pi} \right)^\epsilon \int dp^+ d^{d-2} p_\perp \int \frac{d^d k}{(2\pi)^d} \delta(k^+ - x_2 P_A^+)$$

$$\begin{aligned}
& \times \delta(p^+ - x_3 P_A^+) \delta^{(d-2)}(p_\perp - k_{3\perp}) \text{Tr} \left[(i\gamma_\perp^\nu \gamma^+) (-i)(k^+ g_{\nu\mu} - k_\nu n_\mu) T^a \frac{i(p-k) \cdot \gamma}{(p-k)^2 + i\varepsilon} \right. \\
& \left. \times (-ig_s \gamma_\alpha T^a) \frac{-ig^{\mu\alpha}}{k^2 + i\varepsilon} \mathcal{M}(p) \right].
\end{aligned} \tag{15}$$

Here

$$\mathcal{M}(p) = \int \frac{d^{d-1}\xi}{(2\pi)^{d-1}} e^{-i\xi \cdot p} \langle h_A | \bar{\psi}_+(\xi) \psi_+(0) | h_A \rangle \Big|_{\xi^+=0}. \tag{16}$$

Using the decomposition in Eq.(12), we derive

$$\begin{aligned}
h(x_1, x_2, k_{3\perp}) \Big|_{3a} &= \frac{ig_s^2 C_F}{2(d-2)x_3 M_A^2} \left(\frac{\mu^2 e^{\gamma_E}}{4\pi} \right)^\epsilon \int \frac{d^d k}{(2\pi)^d} \delta(k^+ - x_2 P_A^+) \frac{1}{k^2 + i\varepsilon} \\
&\times \text{Tr} \left[\gamma_\perp^\nu \gamma^+ (k^+ g_{\nu\mu} - k_\nu n_\mu) \frac{(k_3 - k) \cdot \gamma}{(k_3 - k)^2 + i\varepsilon} \gamma_\alpha \gamma_\rho \gamma^- k_{3\perp}^\rho g^{\mu\alpha} \right] \\
&\times h_1^\perp(x_3, k_{3\perp}),
\end{aligned} \tag{17}$$

with $k_3^\mu = (x_3 P_A^+, 0, k_{3\perp})$, $C_F = (N_c^2 - 1)/(2N_c)$, $C_A = N_c$. We find f_1 has no contribution.

Expanding the expression in the trace in k_{3T}^2 and taking the NLP term, we have

$$\begin{aligned}
h(x_1, x_2, k_{3\perp}) \Big|_{3a} &= \frac{ig_s^2 C_F}{2(d-2)x_3 M_A^2} \left(\frac{\mu^2 e^{\gamma_E}}{4\pi} \right)^\epsilon \int \frac{d^d k}{(2\pi)^d} \delta(k^+ - x_2 P_A^+) \frac{1}{k^2 + i\varepsilon} h_1^\perp(x_3, k_{3\perp}) k_{3T}^2 \\
&\times \left(\frac{\partial}{\partial k_{3T}^2} \text{Tr} \left[\gamma_\perp^\nu \gamma^+ (k^+ g_{\nu\mu} - k_\nu n_\mu) \frac{(k_3 - k) \cdot \gamma}{(k_3 - k)^2 + i\varepsilon} \gamma_\alpha \gamma_\rho \gamma^- k_{3\perp}^\rho g^{\mu\alpha} \right] \Big|_{k_{3\perp}=0} \right) \\
&= \frac{ig_s^2 C_F}{x_3 M_A^2} \left(\frac{\mu^2 e^{\gamma_E}}{4\pi} \right)^\epsilon h_1^\perp(x_3, k_{3\perp}) k_{3T}^2 \int \frac{d^d k}{(2\pi)^d} \delta(k^+ - x_2 P_A^+) \\
&\times \frac{2}{d-2} \left[- \frac{2((d-2)k^+ - 2k_3^+) k_T^2}{(d-2)(k^2 + i\varepsilon)(k^2 - 2k^- k_3^+ + i\varepsilon)^2} \right. \\
&\quad \left. - \frac{(d-4)k^+}{(k^2 + i\varepsilon)(k^2 - 2k^- k_3^+ + i\varepsilon)} \right].
\end{aligned} \tag{18}$$

We first carry out the integration over k^- . The denominators contain two singularities in the k^- plane:

$$k_{(1)}^- = \frac{k_T^2 - i\varepsilon}{-2(k_3^+ - k^+)}, \quad k_{(2)}^- = \frac{k_T^2 - i\varepsilon}{2k^+}. \tag{19}$$

Only when $0 < k^+ < k_3^+$, the singularities are on opposite sides of the real axis, which can give a none vanished value for the contour integral of k^- . In this case, we close the integration contour at ∞ in the lower half-plane and take the residue at the point $k^- = k_{(2)}^-$.

Then we obtain

$$h(x_1, x_2, k_{3\perp}) \Big|_{3a} = \frac{2\alpha_s C_F}{x_3 M_A^2} \frac{x_1 x_2}{x_3^2} h_1^\perp(x_3, k_{3\perp}) k_{3T}^2 \frac{1}{4\pi} \left(\frac{1}{\epsilon_{\text{UV}}} - \frac{1}{\epsilon_{\text{IR}}} \right). \tag{20}$$

Here we have used

$$\mu^{2\epsilon} \int \frac{d^{d-2}k_{\perp}}{(2\pi)^{d-2}} \frac{1}{k_T^2} = \frac{1}{4\pi} \left(\frac{1}{\epsilon_{UV}} - \frac{1}{\epsilon_{IR}} \right). \quad (21)$$

In a similar way, we can calculate the contributions from Fig.3(b) and Fig.3(c), we obtain

$$h(x_1, x_2, k_{3\perp}) \Big|_{3b} = - \frac{2\alpha_s C_F}{x_3 M_A^2} \frac{x_1 x_2}{x_3^2} h_1^{\perp}(x_3, k_{3\perp}) k_{3T}^2 \frac{1}{4\pi} \left(\frac{1}{\epsilon_{UV}} - \frac{1}{\epsilon_{IR}} \right), \quad (22a)$$

$$h(x_1, x_2, k_{3\perp}) \Big|_{3c} = 0. \quad (22b)$$

We find that the sum of the three diagrams is zero. Therefore, the contribution from the twist-2 quark-quark correlation function at one-loop vanishes. Consequently, there is no mixing with the quark-quark correlation function at $\mathcal{O}(\alpha_s)$.

Now we turn to the contributions from twist-3 quark-gluon-quark correlation function. The contributions from the quark or gluon self-energy correction are showed in Fig. 4. The

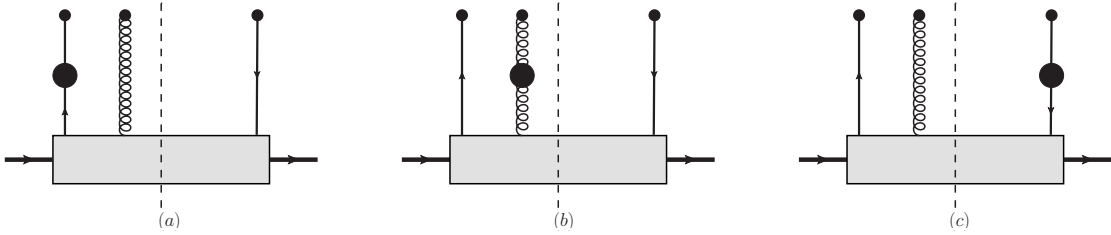


FIG. 4. A set of diagrams for the contributions from twist-3 quark-gluon-quark correlation function. This set only contains the self-energy corrections. The black disk includes the one loop quark or gluon self-energy.

renormalization factors of these diagrams are well-known. Taking the renormalization of g_s in the definition of Φ_F^μ into account, we have

$$h(x_1, x_2, k_{3\perp}) \Big|_{\text{Fig.4, UV}} = \frac{\alpha_s}{4\pi} (-C_F - C_A) \left(\frac{1}{\epsilon_{UV}} + \ln \mu^2 \right) h(x_1, x_2, k_{3\perp}). \quad (23)$$

It is convenient to derive the evolution equations in b -space. In b -space we have

$$\tilde{h}(x_1, x_2, b_{\perp}) \Big|_{\text{Fig.4, UV}} = \frac{\alpha_s}{4\pi} (-C_F - C_A) \left(\frac{1}{\epsilon_{UV}} + \ln \mu^2 \right) \tilde{h}(x_1, x_2, b_{\perp}). \quad (24)$$

The remaining diagrams are given in Fig. 5. Here only the diagrams contain UV or rapidity divergences are included. We will first derive the $1/\epsilon_{IR}$ (IR) divergences of these

diagrams, where the rapidity divergences associated with the IR divergences do not need to be regularized, as they will cancel out between the virtual and real corrections. Next, we derive the total $1/\epsilon$ divergences and rapidity divergences of these diagrams, where the rapidity divergences are regularized using the exponential regulator. By using the results containing $1/\epsilon$ and rapidity divergences to subtract the results containing $1/\epsilon_{\text{IR}}$ divergences, we obtain the $1/\epsilon_{\text{UV}}$ (UV) divergences and the regularized rapidity divergences of these diagrams.

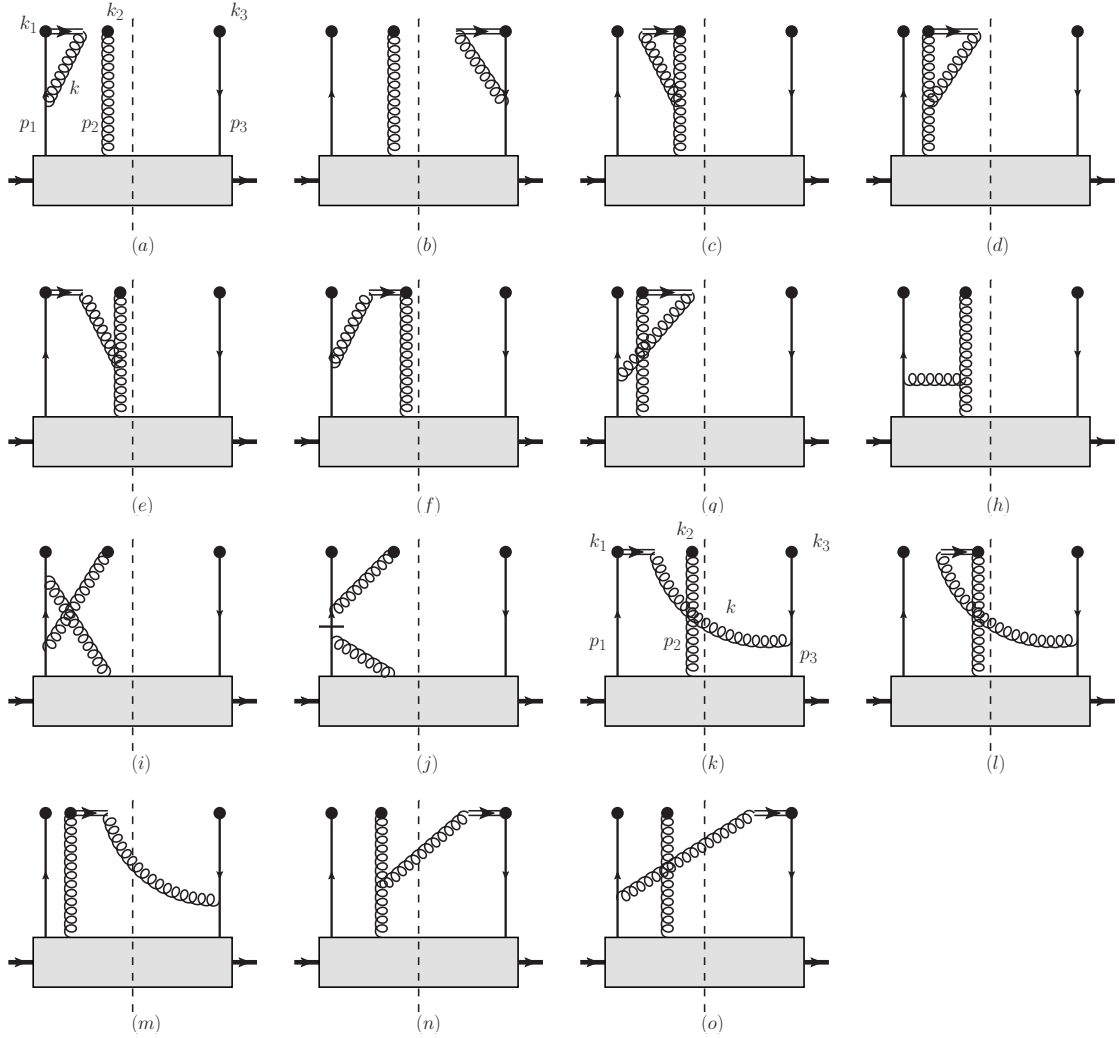


FIG. 5. Another set of diagrams for the contributions from twist-3 quark-gluon-quark correlation function.

We first consider the Fig. 5(a), we have

$$\begin{aligned}
h(x_1, x_2, k_{3\perp}) \Big|_{5a} &= \frac{ig_s}{(d-2)x_3M_A} \left(\frac{\mu^2 e^{\gamma_E}}{4\pi} \right)^\epsilon \int dp_2^+ d^{d-2}p_{2\perp} dp_3^+ d^{d-2}p_{3\perp} \int \frac{d^d k}{(2\pi)^d} \\
&\times \delta(p_2^+ - x_2 P_A^+) \delta(p_3^+ - x_3 P_A^+) \delta^{(d-2)}(p_{3\perp} - k_{3\perp}) \text{Tr} \left[(i\gamma_\perp^\nu \gamma^+) (-i)(k_2^+ g_{\nu\mu} - k_{2\nu} n_\mu) \right. \\
&\times T^b (-ig_s T^a) \frac{in^\rho}{-k^+ + i\varepsilon} \frac{i(p_1 - k) \cdot \gamma}{(p_1 - k)^2 + i\varepsilon} (-ig_s \gamma_\rho T^a) \frac{-i}{k^2 + i\varepsilon} \mathcal{M}_A^{b,\mu}(p_2, p_3) \Big]. \quad (25)
\end{aligned}$$

Here

$$\mathcal{M}_A^{b,\mu}(p_2, p_3) = \int \frac{d^{d-1}\zeta}{(2\pi)^{d-1}} \frac{d^{d-1}\xi}{(2\pi)^{d-1}} e^{-i\xi \cdot p_3 + i\zeta \cdot p_2} \langle h_A | \bar{\psi}_+(\xi) A^{b,\mu}(\zeta) \psi_+(0) | h_A \rangle \Big|_{\xi^+=0, \zeta^+=0}. \quad (26)$$

In above equations, the momentum scale as $p_i^\mu \sim P_A^+(1, \lambda^2, \lambda)$, $k_i^\mu \sim P_A^+(1, \lambda^2, \lambda)$, ($i = 1, 2, 3$), with $\lambda \sim k_{3\perp}/P_A^+$. The collinear gluon scale as $A^{b,\mu} \sim P_A^+(1, \lambda^2, \lambda)$. At NLP, both $A^{b,+}$ and $A_\perp^{b,\mu}$ have contributions. And they were converted to field strength $G^{b,+\mu}$ through partial integration. For simplify, here we only calculate the contribution of A_\perp^b . And this should not affect the final result. In calculating the A_\perp^b contribution, we expand the expression in the square brackets in λ to NLP. We then have

$$\begin{aligned}
h(x_1, x_2, k_{3\perp}) \Big|_{5a} &= \frac{iC_F}{(d-2)x_3M_A} \left(\frac{\mu^2 e^{\gamma_E}}{4\pi} \right)^\epsilon \int \frac{d^d k}{(2\pi)^d} \text{Tr} \left[(i\gamma_\perp^\nu \gamma^+) (-i)(k_2^+ g_{\nu\mu} - \hat{k}_{2\nu} n_\mu) \right. \\
&\times (-ig_s) \frac{in^\rho}{-k^+ + i\varepsilon} \frac{i(\hat{p}_1 - k) \cdot \gamma}{(\hat{p}_1 - k)^2 + i\varepsilon} (-ig_s \gamma_\rho) \frac{-i}{k^2 + i\varepsilon} \frac{1}{k_2^+} \Phi_F^\mu(x_1, x_2, k_{3\perp}) \Big]. \quad (27)
\end{aligned}$$

with $\hat{p}_i^\mu = (p_i^+, 0, 0_\perp)$, $\hat{k}_i^\mu = (k_i^+, 0, 0_\perp)$, $i = 1, 2, 3$. Inserting the parameterization of Φ_F^μ into above equation, we find only h has contribution, which reads

$$\begin{aligned}
h(x_1, x_2, k_{3\perp}) \Big|_{5a} &= \frac{iC_F}{4(d-2)} \left(\frac{\mu^2 e^{\gamma_E}}{4\pi} \right)^\epsilon \int \frac{d^d k}{(2\pi)^d} \frac{1}{k_2^+} \text{Tr} \left[(i\gamma_\perp^\nu \gamma^+) (-i)(k_2^+ g_{\nu\mu} - \hat{k}_{2\nu} n_\mu) \right. \\
&\times (-ig_s) \frac{in^\rho}{-k^+ + i\varepsilon} \frac{i(\hat{p}_1 - k) \cdot \gamma}{(\hat{p}_1 - k)^2 + i\varepsilon} (-ig_s \gamma_\rho) \frac{-i}{k^2 + i\varepsilon} (i\gamma_\perp^\mu \gamma^-) \Big] h(x_1, x_2, k_{3\perp}). \quad (28)
\end{aligned}$$

We first integrate over k^- using contour integration. We then perform the integration over k_\perp using Eq. (21). Finally, we obtain

$$h(x_1, x_2, k_{3\perp}) \Big|_{5a} = 2\alpha_s C_F \left(1 - \ln x_1 - \int_0^1 dy \frac{1}{y - i\varepsilon} \right) \frac{1}{4\pi} \left(\frac{1}{\epsilon_{UV}} - \frac{1}{\epsilon_{IR}} \right) h(x_1, x_2, k_{3\perp}). \quad (29)$$

Employing the identity

$$\int_0^1 dy \frac{1}{y \pm i\varepsilon} = \int_0^1 dy \left(\frac{1}{y} \mp \frac{i\pi}{2} \delta(y) \right), \quad (30)$$

we have

$$h(x_1, x_2, k_{3\perp}) \Big|_{5a} = 2\alpha_s C_F \left(1 - \ln x_1 - \int_0^1 dy \frac{1}{y} - \frac{i\pi}{2}\right) \frac{1}{4\pi} \left(\frac{1}{\epsilon_{UV}} - \frac{1}{\epsilon_{IR}}\right) h(x_1, x_2, k_{3\perp}). \quad (31)$$

In b -space, the result reads

$$\tilde{h}(x_1, x_2, b_\perp) \Big|_{5a} = 2\alpha_s C_F \left(1 - \ln x_1 - \int_0^1 dy \frac{1}{y} - \frac{i\pi}{2}\right) \frac{1}{4\pi} \left(\frac{1}{\epsilon_{UV}} - \frac{1}{\epsilon_{IR}}\right) \tilde{h}(x_1, x_2, b_\perp). \quad (32)$$

The result contain a divergence in the integral of y . This divergence is the rapidity divergence.

Similarly, for Fig. 5(b)-(j), we derive

$$\tilde{h}(x_1, x_2, b_\perp) \Big|_{5b} = 2\alpha_s C_F \left(1 - \ln(x_1 + x_2) - \int_0^1 dy \frac{1}{y} + \frac{i\pi}{2}\right) \frac{1}{4\pi} \left(\frac{1}{\epsilon_{UV}} - \frac{1}{\epsilon_{IR}}\right) \tilde{h}(x_1, x_2, b_\perp), \quad (33a)$$

$$\tilde{h}(x_1, x_2, b_\perp) \Big|_{5c} = \alpha_s \frac{C_A}{2} \left(1 - 2\ln x_2 - \int_0^1 dy \frac{2}{y} - i\pi\right) \frac{1}{4\pi} \left(\frac{1}{\epsilon_{UV}} - \frac{1}{\epsilon_{IR}}\right) \tilde{h}(x_1, x_2, b_\perp), \quad (33b)$$

$$\tilde{h}(x_1, x_2, b_\perp) \Big|_{5d} = \alpha_s \frac{C_A}{2} \left(1 - 2\ln x_2 - \int_0^1 dy \frac{2}{y} - i\pi\right) \frac{1}{4\pi} \left(\frac{1}{\epsilon_{UV}} - \frac{1}{\epsilon_{IR}}\right) \tilde{h}(x_1, x_2, b_\perp), \quad (33c)$$

$$\begin{aligned} \tilde{h}(x_1, x_2, b_\perp) \Big|_{5e} &= \alpha_s \frac{C_A}{2} \left[\int_{-\infty}^{\infty} dy_2 \theta(y_2 - x_2) \frac{x_2(x_2 + y_2)}{(y_2 - x_2)y_2^2} \tilde{h}(y_1, y_2, b_\perp) + i\pi \tilde{h}(x_1, x_2, b_\perp) \right] \\ &\times \frac{1}{4\pi} \left(\frac{1}{\epsilon_{UV}} - \frac{1}{\epsilon_{IR}}\right), \end{aligned} \quad (33d)$$

$$\begin{aligned} \tilde{h}(x_1, x_2, b_\perp) \Big|_{5f} &= 2\alpha_s C_F \left[\int_{-\infty}^{\infty} dy_2 \theta(x_2 - y_2) \frac{x_1 x_2}{(x_2 - y_2)y_1 y_2} \tilde{h}(y_1, y_2, b_\perp) + \frac{i\pi}{2} \tilde{h}(x_1, x_2, b_\perp) \right] \\ &\times \frac{1}{4\pi} \left(\frac{1}{\epsilon_{UV}} - \frac{1}{\epsilon_{IR}}\right), \end{aligned} \quad (33e)$$

$$\begin{aligned} \tilde{h}(x_1, x_2, b_\perp) \Big|_{5g} &= 2\alpha_s \left(C_F - \frac{C_A}{2}\right) \left[\int_{-\infty}^{\infty} dy_2 \theta(x_2 - y_2) \frac{-x_1 x_2}{(x_2 - y_2)y_1 y_2} \tilde{h}(y_1, y_2, b_\perp) \right. \\ &\left. - \frac{i\pi}{2} \tilde{h}(x_1, x_2, b_\perp) \right] \frac{1}{4\pi} \left(\frac{1}{\epsilon_{UV}} - \frac{1}{\epsilon_{IR}}\right), \end{aligned} \quad (33f)$$

$$\begin{aligned} \tilde{h}(x_1, x_2, b_\perp) \Big|_{5h} &= 2\alpha_s \left(\frac{C_A}{2}\right) \int_{-\infty}^{\infty} dy_2 \left[\theta(x_2 - y_2) \frac{x_1(x_2 - y_1)}{(y_1 + y_2)y_1 y_2} + \theta(y_2 - x_2) \right. \\ &\left. \times \frac{x_2(2x_2 - y_1 + y_2)}{2(y_1 + y_2)y_2^2} \right] \frac{1}{4\pi} \left(\frac{1}{\epsilon_{UV}} - \frac{1}{\epsilon_{IR}}\right) \tilde{h}(y_1, y_2, b_\perp), \end{aligned} \quad (33g)$$

$$\begin{aligned} \tilde{h}(x_1, x_2, b_\perp) \Big|_{5i} &= 2\alpha_s \left(C_F - \frac{C_A}{2}\right) \int_{-\infty}^{\infty} dy_2 \left[\theta(y_2 - x_1) \frac{-x_1(x_2 - y_1)}{(y_1 + y_2)y_2^2} - \theta(x_1 - y_2) \right. \\ &\left. \times \frac{x_2(x_2 - y_1)}{(y_1 + y_2)y_1 y_2} \right] \frac{1}{4\pi} \left(\frac{1}{\epsilon_{UV}} - \frac{1}{\epsilon_{IR}}\right) \tilde{h}(y_1, y_2, b_\perp), \end{aligned} \quad (33h)$$

$$\tilde{h}(x_1, x_2, b_\perp) \Big|_{5j} = 2\alpha_s C_F \int_{-\infty}^{\infty} dy_2 \frac{-x_1 x_2}{(y_1 + y_2)^2 y_2} \frac{1}{4\pi} \left(\frac{1}{\epsilon_{UV}} - \frac{1}{\epsilon_{IR}}\right) \tilde{h}(y_1, y_2, b_\perp). \quad (33i)$$

Here we defined $p_1^+ = y_1 P_A^+$, $p_2^+ = y_2 P_A^+$. For these virtual diagrams, we have $y_1 + y_2 = x_1 + x_2 = x_3$. The contributions of Fig. 5(e)-(g) contain the rapidity divergence at $x_2 = y_2$.

The real diagrams Fig. 5(k)-(o) have no UV divergence, but they contain rapidity divergences. For Fig. 5(k), we have

$$\begin{aligned}
h(x_1, x_2, k_{3\perp}) \Big|_{5k} &= \frac{ig_s}{(d-2)x_3 M_A} \left(\frac{\mu^2 e^{\gamma_E}}{4\pi} \right)^\epsilon \int dp_2^+ d^{d-2} p_{2\perp} dp_3^+ d^{d-2} p_{3\perp} \int \frac{d^d k}{(2\pi)^d} \\
&\times \delta(p_2^+ - x_2 P_A^+) \delta(p_3^+ - k^+ - x_3 P_A^+) \delta^{(d-2)}(p_{3\perp} - k_{3\perp} - k_\perp) \text{Tr} \left[(i\gamma_\perp^\nu \gamma^+) (-i) \right. \\
&\times (k_2^+ g_{\nu\mu} - k_{2\nu} n_\mu) T^b (-ig_s T^a) \frac{in^\rho}{k^+ + i\varepsilon} \mathcal{M}_A^{b,\mu}(p_2, p_3) (ig_s \gamma_\rho T^a) \frac{-i(p_3 - k) \cdot \gamma}{(p_3 - k)^2 - i\varepsilon} \Big] \\
&\times (-2\pi) \delta(k^2) \theta(k^+).
\end{aligned} \tag{34}$$

Which result in

$$\begin{aligned}
h(x_1, x_2, k_{3\perp}) \Big|_{5k} &= \frac{i(x_2 + y_1)}{4(d-2)(x_2 + x_1)} \left(C_F - \frac{C_A}{2} \right) \left(\frac{\mu^2 e^{\gamma_E}}{4\pi} \right)^\epsilon \int \frac{d^d k}{(2\pi)^d} \frac{1}{k_2^+} \text{Tr} \left[(i\gamma_\perp^\nu \gamma^+) \right. \\
&\times (-i) (k_2^+ g_{\nu\mu} - \hat{k}_{2\nu} n_\mu) (-ig_s) \frac{in^\rho}{k^+ + i\varepsilon} (i\gamma_\perp^\mu \gamma^-) (ig_s \gamma_\rho) \frac{-i(\hat{p}_3 - k) \cdot \gamma}{(\hat{p}_3 - k)^2 - i\varepsilon} \Big] \\
&\times (-2\pi) \delta(k^2) \theta(k^+) h(y_1, x_2, k_{3\perp} + k_\perp).
\end{aligned} \tag{35}$$

Here still only h contributes. We integrate over k^- and obtain

$$\begin{aligned}
h(x_1, x_2, k_{3\perp}) \Big|_{5k} &= 2\alpha_s \left(C_F - \frac{C_A}{2} \right) \int_{x_1}^\infty dy_1 \left(\frac{1}{y_1 - x_1} - \frac{i\pi}{2} \delta(y_1 - x_1) \right) \\
&\times \left(\frac{\mu^2 e^{\gamma_E}}{4\pi} \right)^\epsilon \int \frac{d^{2-2\epsilon} k_\perp}{(2\pi)^{2-2\epsilon}} \frac{1}{k_T^2} h(y_1, x_2, k_{3\perp} + k_\perp).
\end{aligned} \tag{36}$$

The result contains the rapidity divergence at $x_1 = y_1$ and IR divergence at $k_\perp = 0$. According to [18]

$$\frac{\mu^{2\epsilon}}{\pi^{1-\epsilon}} \int \frac{d^{2-2\epsilon} k_\perp}{k_T^{2+2\delta}} e^{ik_\perp \cdot b_\perp} = \mu^{2\epsilon} e^{-2(\epsilon+\delta)\gamma_E} \frac{\Gamma(-\epsilon-\delta)}{\Gamma(1+\delta)} \left(\frac{b_T^2}{4e^{-2\gamma_E}} \right)^{\epsilon+\delta}, \tag{37}$$

we have

$$\frac{(4\pi)^\epsilon \mu^{2\epsilon}}{\pi^{1-\epsilon}} \int \frac{d^{2-2\epsilon} k_\perp}{k_T^2} e^{ik_\perp \cdot b_\perp} = \left(\frac{4\pi b_T^2 \mu^2}{4} \right)^\epsilon \Gamma(-\epsilon), \tag{38a}$$

$$-\frac{(4\pi)^\epsilon \mu^{2\epsilon}}{\pi^{1-\epsilon}} \int \frac{d^{2-2\epsilon} k_\perp}{k_T^2} \ln k_T^2 e^{ik_\perp \cdot b_\perp} = \left(\frac{4\pi b_T^2 \mu^2}{4} \right)^\epsilon \Gamma(-\epsilon) \left(-\psi(-\epsilon) + \ln \frac{b_T^2}{4} + \gamma_E \right), \tag{38b}$$

where $\psi(x) = \Gamma'(x)/\Gamma(x)$. Applying above equations, we can convert Eq. (36) into a form in b -space,

$$\tilde{h}(x_1, x_2, b_\perp) \Big|_{5k} = 2\alpha_s \left(C_F - \frac{C_A}{2} \right) \int_{x_1}^\infty dy_1 \left(\frac{1}{y_1 - x_1} - \frac{i\pi}{2} \delta(y_1 - x_1) \right) \frac{1}{4\pi} \left(-\frac{1}{\epsilon_{\text{IR}}} - \ln \mu^2 \right)$$

$$\times \tilde{h}(y_1, x_2, b_\perp) + \dots . \quad (39)$$

Here \dots denote the finite terms that are irrelevant. Similarly, for Fig. 5(l)-(o) we can derive

$$\begin{aligned} \tilde{h}(x_1, x_2, b_\perp) \Big|_{5l} &= 2\alpha_s \left(C_F - \frac{C_A}{2} \right) \int_{x_2}^{\infty} dy_2 \left(\frac{-x_2}{(y_2 - x_2)y_2} + \frac{i\pi}{2} \delta(y_2 - x_2) \right) \\ &\times \frac{1}{4\pi} \left(-\frac{1}{\epsilon_{\text{IR}}} - \ln \mu^2 \right) \tilde{h}(x_1, y_2, b_\perp) + \dots , \end{aligned} \quad (40a)$$

$$\begin{aligned} \tilde{h}(x_1, x_2, b_\perp) \Big|_{5m} &= 2\alpha_s C_F \int_{x_2}^{\infty} dy_2 \left(\frac{x_2}{(y_2 - x_2)y_2} - \frac{i\pi}{2} \delta(y_2 - x_2) \right) \\ &\times \frac{1}{4\pi} \left(-\frac{1}{\epsilon_{\text{IR}}} - \ln \mu^2 \right) \tilde{h}(x_1, y_2, b_\perp) + \dots , \end{aligned} \quad (40b)$$

$$\begin{aligned} \tilde{h}(x_1, x_2, b_\perp) \Big|_{5n} &= \alpha_s \frac{C_A}{2} \int_{x_2}^{\infty} dy_2 \left(\frac{x_2(x_2 + y_2)(x_1 + y_2)}{(y_2 - x_2)(x_1 + x_2)y_2^2} + i\pi \delta(y_2 - x_2) \right) \\ &\times \frac{1}{4\pi} \left(-\frac{1}{\epsilon_{\text{IR}}} - \ln \mu^2 \right) \tilde{h}(x_1, y_2, b_\perp) + \dots , \end{aligned} \quad (40c)$$

$$\begin{aligned} \tilde{h}(x_1, x_2, b_\perp) \Big|_{5o} &= 2\alpha_s \left(C_F - \frac{C_A}{2} \right) \int_{x_1}^{\infty} dy_1 \left(\frac{x_1(y_1 + x_2)}{(y_1 - x_1)y_1(x_1 + x_2)} + \frac{i\pi}{2} \delta(y_1 - x_1) \right) \\ &\times \frac{1}{4\pi} \left(-\frac{1}{\epsilon_{\text{IR}}} - \ln \mu^2 \right) \tilde{h}(y_1, x_2, b_\perp) + \dots . \end{aligned} \quad (40d)$$

Summing up the IR divergences in Eqs.(32), (33), (39) and (40), we have

$$\begin{aligned} &\tilde{h}(x_1, x_2, b_\perp) \Big|_{\text{Fig.5, IR}} \\ &= \frac{2\alpha_s}{4\pi} \left\{ \left[2C_F + \frac{C_A}{2} + \left(C_F - \frac{C_A}{2} \right) \left(-\ln \frac{x_1 + x_2}{x_1} \right) + \frac{C_A}{2} \left(-\ln \frac{x_1 + x_2}{x_2} \right) \right] \tilde{h}(x_1, x_2, b_\perp) \right. \\ &\quad + \frac{C_A}{2} \left[2 \int_{x_2}^{\infty} dy_2 \left[\frac{x_2}{(y_2 - x_2)y_2} \right]_+ + \int_{x_2}^{\infty} dy_2 \frac{x_2(y_2 - x_1)}{2y_2^2(x_1 + x_2)} \right] \tilde{h}(x_1, y_2, b_\perp) \\ &\quad + \left(C_F - \frac{C_A}{2} \right) \left[2 \int_{x_1}^{\infty} dy_1 \left[\frac{x_1}{(y_1 - x_1)y_1} \right]_+ + \int_{x_1}^{\infty} dy_1 \left(\frac{2}{y_1} - \frac{x_2}{y_1(x_2 + x_1)} \right) \right] \tilde{h}(y_1, x_2, b_\perp) \\ &\quad + \frac{C_A}{2} \left[\int_{-\infty}^{\infty} dy_2 \left(\theta(x_2 - y_2) \frac{x_1(x_2 + y_2)}{(y_1 + y_2)y_1 y_2} + \theta(y_2 - x_2) \frac{x_2(x_2 + y_2)}{(y_1 + y_2)y_2^2} \right) \tilde{h}(y_1, y_2, b_\perp) \right. \\ &\quad + \int_{x_1}^{\infty} dy_1 \frac{x_1}{(y_1 - x_1)y_1} \left(\tilde{h}(y_1, y_2, b_\perp) - \tilde{h}(x_1, x_2, b_\perp) \right) \\ &\quad + \left. \int_{x_2}^{\infty} dy_2 \left(\frac{x_2^2}{(y_2 - x_2)y_2^2} \tilde{h}(y_1, y_2, b_\perp) - \frac{x_2}{(y_2 - x_2)y_2} \tilde{h}(x_1, x_2, b_\perp) \right) \right] \\ &\quad + \left(C_F - \frac{C_A}{2} \right) \int_{-\infty}^{\infty} dy_2 \left[\theta(y_2 - x_1) \frac{-x_1(x_2 - y_1)}{(y_1 + y_2)y_2^2} - \theta(x_1 - y_2) \frac{x_2(x_2 - y_1)}{(y_1 + y_2)y_2 y_1} \right] \\ &\quad \times \tilde{h}(y_1, y_2, b_\perp) + C_F \int_{-\infty}^{\infty} dy_2 \frac{-x_1 x_2}{(y_1 + y_2)^2 y_2} \tilde{h}(y_1, y_2, b_\perp) \left. \right\} \left(-\frac{1}{\epsilon_{\text{IR}}} - \ln \mu^2 \right). \end{aligned} \quad (41)$$

To derive above result, we have used following relations

$$\int_{x_1}^{\infty} dy_1 \frac{x_1}{y_1(y_1 - x_1)} = \int_0^1 dy \frac{1}{1-y} + \ln x_1 = \int_0^1 dy \frac{1}{y} + \ln x_1, \quad (42a)$$

$$\int_{x_2}^{\infty} dy_2 \frac{x_2}{y_2(y_2 - x_2)} = \int_0^1 dy \frac{1}{1-y} + \ln x_2 = \int_0^1 dy \frac{1}{y} + \ln x_2. \quad (42b)$$

In Eq. (41), we find the rapidity divergences associated with $1/\epsilon_{\text{IR}}$ are cancelled. After this cancellation, the plus-distribution appears, which is defined as

$$\int_x^{\infty} dy [f(y-x)]_+ g(y) = \int_x^{\infty} dy f(y-x) (g(y) - g(x)). \quad (43)$$

In addition, we find the imaginary parts are also cancelled.

We now derive the total $1/\epsilon$ divergences and rapidity divergences of the diagrams in Fig. 5. The contributions from the virtual diagrams vanish due to the cancellation between $1/\epsilon_{\text{UV}}$ and $1/\epsilon_{\text{IR}}$. Therefore, we only need to consider the real diagrams in Fig. 5(k)-(o). To regularize the rapidity divergences, we use the exponential regulator. This regulator is introduced by multiplying the phase space measure in Eq.(34) by an exponential factor:

$$\int \frac{d^d k}{(2\pi)^d} (2\pi) \delta(k^2) \rightarrow \lim_{\tau \rightarrow 0} \int \frac{d^d k}{(2\pi)^d} (2\pi) \delta(k^2) \exp(-b_0 \tau (k^+ + k^-)), \quad (44)$$

with $b_0 = 2e^{-\gamma_E}$. For Fig. 5(k), the exponential factor can be rewritten as

$$\exp(-b_0 \tau (k^+ + k^-)) = \exp \left[-b_0 \tau \left((y_1 - x_1) P_A^+ + \frac{k_T^2}{2(y_1 - x_1) P_A^+} \right) \right]. \quad (45)$$

We can drop the term proportional to $\tau(y_1 - x_1)$, as it has no contribution in the limit $\tau \rightarrow 0$. We then have

$$\begin{aligned} h(x_1, x_2, k_{3\perp}) \Big|_{5k} &= 2\alpha_s \left(C_F - \frac{C_A}{2} \right) \left(\frac{\mu^2 e^{\gamma_E}}{4\pi} \right)^\epsilon \int \frac{d^{2-2\epsilon} k_\perp}{(2\pi)^{2-2\epsilon}} \frac{1}{k_T^2} \int dy_1 \left[\frac{1}{y_1 - x_1} \right. \\ &\quad \times \exp \left[\frac{-b_0 \tau k_T^2}{2(y_1 - x_1) P_A^+} \right] - \frac{i\pi}{2} \delta(y_1 - x_1) \Big] h(y_1, x_2, k_{3\perp} + k_\perp). \end{aligned} \quad (46)$$

The term in the exponent provides the service of regularizing the rapidity divergence. Using

$$\frac{x_1}{(y_1 - x_1)y_1} \exp \left[\frac{-b_0 \tau k_T^2}{2(y_1 - x_1) P_A^+} \right] = -\ln \left(\frac{\tau k_T^2}{x_1 P_A^+} \right) \delta(y_1 - x_1) + \left[\frac{x_1}{(y_1 - x_1)y_1} \right]_+ + \mathcal{O}(\tau), \quad (47)$$

we obtain

$$h(x_1, x_2, k_{3\perp}) \Big|_{5k} = 2\alpha_s \left(C_F - \frac{C_A}{2} \right) \left(\frac{\mu^2 e^{\gamma_E}}{4\pi} \right)^\epsilon \int \frac{d^{2-2\epsilon} k_\perp}{(2\pi)^{2-2\epsilon}} \frac{1}{k_T^2} \left\{ \int_{x_1}^{\infty} dy_1 \left(-\ln \frac{\tau k_T^2}{x_1 P_A^+} \right) \right.$$

$$\begin{aligned}
& \times \delta(y_1 - x_1) + \left[\frac{x_1}{(y_1 - x_1)y_1} \right]_+ \Big) + \int_{x_1}^{\infty} dy_1 \left(\frac{1}{y_1} - \frac{i\pi}{2} \delta(y_1 - x_1) \right) \Big\} \\
& \times h(y_1, x_2, k_{3\perp} + k_{\perp}).
\end{aligned} \tag{48}$$

We find the rapidity divergences are regulated by regulator τ . Applying Eq.(38), we derive

$$\begin{aligned}
\tilde{h}(x_1, x_2, b_{\perp}) \Big|_{5k} &= 2\alpha_s \left(C_F - \frac{C_A}{2} \right) \left\{ \int_{x_1}^{\infty} dy_1 \left[-\ln \frac{\tau}{x_1 P_A^+} \delta(y_1 - x_1) + \left[\frac{x_1}{(y_1 - x_1)y_1} \right]_+ \right. \right. \\
&+ \left. \frac{1}{y_1} - \frac{i\pi}{2} \delta(y_1 - x_1) \right] \frac{1}{4\pi} \left(-\frac{1}{\epsilon} - \ln \frac{b_T^2 \mu^2}{4e^{-2\gamma_E}} \right) \\
&+ \int_{x_1}^{\infty} dy_1 \delta(y_1 - x_1) \frac{1}{4\pi} \left(\frac{1}{\epsilon^2} + \frac{\ln \mu^2}{\epsilon} + \frac{1}{2} \ln^2 \mu^2 + \dots \right) \Big\} \\
&\times \tilde{h}(y_1, x_2, b_{\perp}).
\end{aligned} \tag{49}$$

Again, the \dots represent finite terms that are not relevant to our study. Similarly, we can derive

$$\begin{aligned}
\tilde{h}(x_1, x_2, b_{\perp}) \Big|_{5l} &= -2\alpha_s \left(C_F - \frac{C_A}{2} \right) \left\{ \int_{x_2}^{\infty} dy_2 \left[-\ln \frac{\tau}{x_2 P_A^+} \delta(y_2 - x_2) + \left[\frac{x_2}{(y_2 - x_2)y_2} \right]_+ \right. \right. \\
&- \left. \frac{i\pi}{2} \delta(y_2 - x_2) \right] \frac{1}{4\pi} \left(-\frac{1}{\epsilon} - \ln \frac{b_T^2 \mu^2}{4e^{-2\gamma_E}} \right) \\
&+ \int_{x_2}^{\infty} dy_2 \delta(y_2 - x_2) \frac{1}{4\pi} \left(\frac{1}{\epsilon^2} + \frac{\ln \mu^2}{\epsilon} + \frac{1}{2} \ln^2 \mu^2 + \dots \right) \Big\} \\
&\times \tilde{h}(x_1, y_2, b_{\perp}),
\end{aligned} \tag{50a}$$

$$\begin{aligned}
\tilde{h}(x_1, x_2, b_{\perp}) \Big|_{5m} &= 2\alpha_s C_F \left\{ \int_{x_2}^{\infty} dy_2 \left[-\ln \frac{\tau}{x_2 P_A^+} \delta(y_2 - x_2) + \left[\frac{x_2}{(y_2 - x_2)y_2} \right]_+ \right. \right. \\
&- \left. \frac{i\pi}{2} \delta(y_2 - x_2) \right] \frac{1}{4\pi} \left(-\frac{1}{\epsilon} - \ln \frac{b_T^2 \mu^2}{4e^{-2\gamma_E}} \right) \\
&+ \int_{x_2}^{\infty} dy_2 \delta(y_2 - x_2) \frac{1}{4\pi} \left(\frac{1}{\epsilon^2} + \frac{\ln \mu^2}{\epsilon} + \frac{1}{2} \ln^2 \mu^2 + \dots \right) \Big\} \\
&\times \tilde{h}(x_1, y_2, b_{\perp}),
\end{aligned} \tag{50b}$$

$$\begin{aligned}
\tilde{h}(x_1, x_2, b_{\perp}) \Big|_{5n} &= 2\alpha_s \left(\frac{C_A}{2} \right) \left\{ \int_{x_2}^{\infty} dy_2 \left[-\ln \frac{\tau}{x_2 P_A^+} \delta(y_2 - x_2) + \left[\frac{x_2}{(y_2 - x_2)y_2} \right]_+ \right. \right. \\
&+ \left. \frac{x_2(y_2 - x_1)}{2y_2^2(x_1 + x_2)} + \frac{i\pi}{2} \delta(y_2 - x_2) \right] \frac{1}{4\pi} \left(-\frac{1}{\epsilon} - \ln \frac{b_T^2 \mu^2}{4e^{-2\gamma_E}} \right) \\
&+ \int_{x_2}^{\infty} dy_2 \delta(y_2 - x_2) \frac{1}{4\pi} \left(\frac{1}{\epsilon^2} + \frac{\ln \mu^2}{\epsilon} + \frac{1}{2} \ln^2 \mu^2 + \dots \right) \Big\} \\
&\times \tilde{h}(x_1, y_2, b_{\perp}),
\end{aligned} \tag{50c}$$

$$\tilde{h}(x_1, x_2, b_{\perp}) \Big|_{5o} = 2\alpha_s \left(C_F - \frac{C_A}{2} \right) \left\{ \int_{x_1}^{\infty} dy_1 \left[-\ln \frac{\tau}{x_1 P_A^+} \delta(y_1 - x_1) + \left[\frac{x_1}{(y_1 - x_1)y_1} \right]_+ \right. \right.$$

$$\begin{aligned}
& + \frac{x_1}{y_1(x_1 + x_2)} + \frac{i\pi}{2}\delta(y_1 - x_1) \Big] \frac{1}{4\pi} \left(-\frac{1}{\epsilon} - \ln \frac{b_T^2 \mu^2}{4e^{-2\gamma_E}} \right) \\
& + \int_{x_1}^{\infty} dy_1 \delta(y_1 - x_1) \frac{1}{4\pi} \left(\frac{1}{\epsilon^2} + \frac{\ln \mu^2}{\epsilon} + \frac{1}{2} \ln^2 \mu^2 + \dots \right) \Big\} \\
& \times \tilde{h}(y_1, x_2, b_{\perp}).
\end{aligned} \tag{50d}$$

We can obtain the total $1/\epsilon$ divergences and rapidity divergences by summing the results in Eqs.(49) and (50). Using this summation to subtract the IR divergences in Eq.(41), we then derive the UV divergences and the regularized rapidity divergences of the diagrams in Fig. 5. Combining the result of Fig. 4 in Eq. (24), we then derive

$$\begin{aligned}
& \tilde{h}(x_1, x_2, b_{\perp}) \Big|_{\text{UV}} \\
& = \frac{4\alpha_s}{4\pi} C_F \left(\frac{1}{\epsilon^2} + \frac{\ln \mu^2}{\epsilon} + \frac{1}{2} \ln^2 \mu^2 \right) \tilde{h}(x_1, x_2, b_{\perp}) \\
& + \frac{2\alpha_s}{4\pi} \left\{ \left[\frac{3}{2} C_F + \left(C_F - \frac{C_A}{2} \right) \left(-\ln \frac{x_1 + x_2}{x_1} \right) + \frac{C_A}{2} \left(-\ln \frac{x_1 + x_2}{x_2} \right) \right] \tilde{h}(x_1, x_2, b_{\perp}) \right. \\
& + \frac{C_A}{2} \left[\int_{-\infty}^{\infty} dy_2 \left[\theta(x_2 - y_2) \frac{x_1(x_2 + y_2)}{(y_1 + y_2)y_1 y_2} + \theta(y_2 - x_2) \frac{x_2(x_2 + y_2)}{(y_1 + y_2)y_2^2} \right] \tilde{h}(y_1, y_2, b_{\perp}) \right. \\
& + \int_{x_1}^{\infty} dy_1 \frac{x_1}{(y_1 - x_1)y_1} \left(\tilde{h}(y_1, y_2, b_{\perp}) - \tilde{h}(x_1, x_2, b_{\perp}) \right) \\
& + \int_{x_2}^{\infty} dy_2 \left(\frac{x_2^2}{(y_2 - x_2)y_2^2} \tilde{h}(y_1, y_2, b_{\perp}) - \frac{x_2}{(y_2 - x_2)y_2} \tilde{h}(x_1, x_2, b_{\perp}) \right) \Big] \\
& + \left(C_F - \frac{C_A}{2} \right) \int_{-\infty}^{\infty} dy_2 \left[\theta(y_2 - x_1) \frac{-x_1(x_2 - y_1)}{(y_1 + y_2)y_2^2} - \theta(x_1 - y_2) \frac{x_2(x_2 - y_1)}{(y_1 + y_2)y_2 y_1} \right] \\
& \times \tilde{h}(y_1, y_2, b_{\perp}) + C_F \int_{-\infty}^{\infty} dy_2 \frac{-x_1 x_2}{(y_1 + y_2)^2 y_2} \tilde{h}(y_1, y_2, b_{\perp}) \Big\} \left(\frac{1}{\epsilon} + \ln \mu^2 \right) \\
& + \frac{2\alpha_s}{4\pi} \left[\frac{C_A}{2} \int_{x_2}^{\infty} dy_2 \left(2 \ln \frac{\tau}{x_2 P_A^+} \delta(y_2 - x_2) \right) \tilde{h}(x_1, y_2, b_{\perp}) + \left(C_F - \frac{C_A}{2} \right) \right. \\
& \times \int_{x_1}^{\infty} dy_1 \left(2 \ln \frac{\tau}{x_1 P_A^+} \delta(y_1 - x_1) \right) \tilde{h}(y_1, x_2, b_{\perp}) \Big] \left(\frac{1}{\epsilon} + \ln \frac{b_T^2 \mu^2}{4e^{-2\gamma_E}} \right).
\end{aligned} \tag{51}$$

With above result, we now can derive the evolution equations for \tilde{h} . The RG evolution equation is given by

$$\frac{d}{d \ln \mu^2} \tilde{h}(x_1, x_2, b_{\perp}) = \left[\frac{\alpha_s C_F}{\pi} \ln \frac{\mu^2}{(x_1 + x_2) \nu P_A^+} + \mathbb{K}_A \right] \tilde{h}(x_1, x_2, b_{\perp}), \tag{52}$$

where $\nu = 1/\tau$, and \mathbb{K}_A is the integral kernel that acts on the TMD PDF, defined by

$$\begin{aligned}
& \mathbb{K}_A \tilde{h}(x_1, x_2, b_{\perp}) \\
& = \frac{\alpha_s}{2\pi} \left\{ \left[\frac{3}{2} C_F + \left(C_F - \frac{C_A}{2} \right) \ln \frac{x_1 + x_2}{x_1} + \frac{C_A}{2} \ln \frac{x_1 + x_2}{x_2} \right] \tilde{h}(x_1, x_2, b_{\perp}) \right.
\end{aligned}$$

$$\begin{aligned}
& + \frac{C_A}{2} \left[\int_{-\infty}^{\infty} dy_2 \left[\theta(x_2 - y_2) \frac{x_1(x_1 + 2x_2)}{(x_1 + x_2)^2 y_1} + \theta(y_2 - x_2) \frac{x_2^2(x_1 + x_2 + y_2)}{(x_1 + x_2)^2 y_2^2} \right] \tilde{h}(y_1, y_2, b_{\perp}) \right. \\
& + \int_{x_1}^{\infty} dy_1 \frac{x_1}{(y_1 - x_1)y_1} \left(\tilde{h}(y_1, y_2, b_{\perp}) - \tilde{h}(x_1, x_2, b_{\perp}) \right) \\
& + \int_{x_2}^{\infty} dy_2 \left(\frac{x_2^2}{(y_2 - x_2)y_2^2} \tilde{h}(y_1, y_2, b_{\perp}) - \frac{x_2}{(y_2 - x_2)y_2} \tilde{h}(x_1, x_2, b_{\perp}) \right) \Big] \\
& + \left(C_F - \frac{C_A}{2} \right) \int_{-\infty}^{\infty} dy_2 \left[\theta(y_2 - x_1) \frac{x_1(x_1^2 + x_1(x_2 - y_2) - 2x_2 y_2)}{(x_1 + x_2)^2 y_2^2} \right. \\
& \left. - \theta(x_1 - y_2) \frac{x_2^2}{(x_1 + x_2)^2 y_1} \right] \tilde{h}(y_1, y_2, b_{\perp}) \Big\}. \tag{53}
\end{aligned}$$

We find our evolution kernel \mathbb{K}_A agrees with the kernel $\Upsilon_{x_1 x_2 x_3} + 2\mathbb{P}_{x_2 x_1}^A$ in Ref.[42], but differs from the kernel $\Upsilon_{x_1 x_2 x_3} + 2\mathbb{P}_{x_2 x_1}^A$ in Ref.[41] by a sign. The evolution equation with respect to the rapidity scale ν is given by

$$\frac{d}{d \ln \nu} \tilde{h}(x_1, x_2, b_{\perp}) = - \frac{\alpha_s C_F}{\pi} \ln \frac{b_T^2 \mu^2}{4e^{-2\gamma_E}} \tilde{h}(x_1, x_2, b_{\perp}). \tag{54}$$

Following the same route, we derive the evolution equations for distributions $f^{\perp} - ig^{\perp}$, $f^{\perp} + ig^{\perp}$ and h^{\perp} . The RG evolution equations read

$$\frac{d}{d \ln \mu^2} (\tilde{f}^{\perp(1)} - i\tilde{g}^{\perp(1)}) = \left[\frac{\alpha_s C_F}{\pi} \ln \frac{\mu^2}{(x_1 + x_2)\nu P_A^+} + \mathbb{K}_A \right] (\tilde{f}^{\perp(1)} - i\tilde{g}^{\perp(1)}), \tag{55a}$$

$$\frac{d}{d \ln \mu^2} (\tilde{f}^{\perp(1)} + i\tilde{g}^{\perp(1)}) = \left[\frac{\alpha_s C_F}{\pi} \ln \frac{\mu^2}{(x_1 + x_2)\nu P_A^+} + \mathbb{K}_B \right] (\tilde{f}^{\perp(1)} + i\tilde{g}^{\perp(1)}), \tag{55b}$$

$$\frac{d}{d \ln \mu^2} \tilde{h}^{\perp(2)} = \left[\frac{\alpha_s C_F}{\pi} \ln \frac{\mu^2}{(x_1 + x_2)\nu P_A^+} + \mathbb{K}_B \right] \tilde{h}^{\perp(2)}, \tag{55c}$$

here the argument of distributions (x_1, x_2, b_{\perp}) is omitted. The evolution kernel \mathbb{K}_B is given by

$$\begin{aligned}
& \mathbb{K}_B \tilde{h}^{\perp(2)}(x_1, x_2, b_{\perp}) \\
& = \frac{\alpha_s}{2\pi} \left\{ \left[\frac{3}{2} C_F + \left(C_F - \frac{C_A}{2} \right) \ln \frac{x_1 + x_2}{x_1} + \frac{C_A}{2} \ln \frac{x_1 + x_2}{x_2} \right] \tilde{h}^{\perp(2)}(x_1, x_2, b_{\perp}) \right. \\
& + \frac{C_A}{2} \left[\int_{x_1}^{\infty} dy_1 \frac{x_1}{(y_1 - x_1)y_1} \left(\tilde{h}^{\perp(2)}(y_1, y_2, b_{\perp}) - \tilde{h}^{\perp(2)}(x_1, x_2, b_{\perp}) \right) \right. \\
& + \int_{x_2}^{\infty} dy_2 \left(\frac{x_2^2}{(y_2 - x_2)y_2^2} \tilde{h}^{\perp(2)}(y_1, y_2, b_{\perp}) - \frac{x_2}{(y_2 - x_2)y_2} \tilde{h}^{\perp(2)}(x_1, x_2, b_{\perp}) \right) \Big] \\
& \left. + \left(C_F - \frac{C_A}{2} \right) \int_{-\infty}^{\infty} dy_2 \theta(y_2 - x_1) \frac{x_1}{y_2^2} \tilde{h}^{\perp(2)}(y_1, y_2, b_{\perp}) \right\}. \tag{56}
\end{aligned}$$

Again, our evolution kernel \mathbb{K}_B differs from the the kernel $\Upsilon_{x_1 x_2 x_3} + 2\mathbb{P}_{x_2 x_1}^B$ in Ref.[41] by a sign. The evolution in the rapidity scale ν is the same for all distributions. It reads

$$\frac{d}{d \ln \nu} H(x_1, x_2, b_{\perp}) = - \frac{\alpha_s C_F}{\pi} \ln \frac{b_T^2 \mu^2}{4e^{-2\gamma_E}} H(x_1, x_2, b_{\perp}), \tag{57}$$

here $H \in \{\tilde{f}^{\perp(1)} - i\tilde{g}^{\perp(1)}, \tilde{f}^{\perp(1)} + i\tilde{g}^{\perp(1)}, \tilde{h}^{\perp(2)}\}$.

V. SOFT SUBTRACTION

For TMD factorization, it is well known that a soft subtraction [5, 10, 11, 36] or a zero-bin subtraction [49] is necessary to avoid double-counting between the collinear sectors and the soft sector. To eliminate double-counting, we divide each TMD PDF by a soft factor. It has been demonstrated in [38] that the soft factor is identical for both the twist-2 and twist-3 TMD PDFs, and is given by the LP soft function

$$\mathcal{S}_{\text{LP}}(b_\perp) = \frac{1}{N_c} \text{Tr} \langle 0 | \mathcal{L}_l(b_\perp) \mathcal{L}_n^\dagger(b_\perp) \mathcal{L}_n(0) \mathcal{L}_l^\dagger(0) | 0 \rangle. \quad (58)$$

We then implement the soft subtraction for twist-3 TMD PDFs by making the following replacements:

$$H(x_1, x_2, b_\perp) \rightarrow \frac{H(x_1, x_2, b_\perp)}{\sqrt{\mathcal{S}_{\text{LP}}(b_\perp)}} = H^{\text{sub}}(x_1, x_2, b_\perp), \quad (59)$$

where $H \in \{\tilde{f}^{\perp(1)} - i\tilde{g}^{\perp(1)}, \tilde{f}^{\perp(1)} + i\tilde{g}^{\perp(1)}, \tilde{h}, \tilde{h}^{\perp(2)}\}$. The exponentially regularized LP soft function has been calculated to N³LO in [14]. According to their result we have

$$\frac{d}{d \ln \mu^2} \mathcal{S}_{\text{LP}}(b_\perp) = \left[\frac{\alpha_s C_F}{\pi} \ln \frac{\mu^2}{\nu^2} + \mathcal{O}(\alpha_s^2) \right] \mathcal{S}_{\text{LP}}(b_\perp), \quad (60a)$$

$$\frac{d}{d \ln \nu} \mathcal{S}_{\text{LP}}(b_\perp) = \left[-\frac{2\alpha_s C_F}{\pi} \ln \frac{b_T^2 \mu^2}{4e^{-2\gamma_E}} + \mathcal{O}(\alpha_s^2) \right] \mathcal{S}_{\text{LP}}(b_\perp). \quad (60b)$$

Based on Eqs. (55), (57) and (60), we immediately obtain the evolution equations for the subtracted distributions $H^{\text{sub}}(x_1, x_2, b_\perp)$. The RG evolution equations read

$$\frac{d}{d \ln \mu^2} (\tilde{f}^{\perp(1),\text{sub}} - i\tilde{g}^{\perp(1),\text{sub}}) = \left[\frac{\alpha_s C_F}{2\pi} \ln \frac{\mu^2}{((x_1 + x_2)P_A^+)^2} + \mathbb{K}_A \right] (\tilde{f}^{\perp(1),\text{sub}} - i\tilde{g}^{\perp(1),\text{sub}}), \quad (61a)$$

$$\frac{d}{d \ln \mu^2} (\tilde{f}^{\perp(1),\text{sub}} + i\tilde{g}^{\perp(1),\text{sub}}) = \left[\frac{\alpha_s C_F}{2\pi} \ln \frac{\mu^2}{((x_1 + x_2)P_A^+)^2} + \mathbb{K}_B \right] (\tilde{f}^{\perp(1),\text{sub}} + i\tilde{g}^{\perp(1),\text{sub}}), \quad (61b)$$

$$\frac{d}{d \ln \mu^2} \tilde{h}^{\text{sub}} = \left[\frac{\alpha_s C_F}{2\pi} \ln \frac{\mu^2}{((x_1 + x_2)P_A^+)^2} + \mathbb{K}_A \right] \tilde{h}^{\text{sub}}, \quad (61c)$$

$$\frac{d}{d \ln \mu^2} \tilde{h}^{\perp(2),\text{sub}} = \left[\frac{\alpha_s C_F}{2\pi} \ln \frac{\mu^2}{((x_1 + x_2)P_A^+)^2} + \mathbb{K}_B \right] \tilde{h}^{\perp(2),\text{sub}}. \quad (61d)$$

These results reproduce the RG evolution equations given in [42] with $\zeta = ((x_1 + x_2)P_A^+)^2$.

For the rapidity scale, we find the ν dependence vanished,

$$\frac{d}{d \ln \nu} H^{\text{sub}}(x_1, x_2, b_\perp) = 0, \quad (62)$$

where $H \in \{\tilde{f}^{\perp(1)} - i\tilde{g}^{\perp(1)}, \tilde{f}^{\perp(1)} + i\tilde{g}^{\perp(1)}, \tilde{h}, \tilde{h}^{\perp(2)}\}$. This indicates that the rapidity divergences cancel in the combination $H^{\text{sub}} = H/\sqrt{\mathcal{S}_{\text{LP}}}$. However, this cancellation leaves a residual dependence on the scale $\zeta = ((x_1 + x_2)P_A^+)^2$, which reads

$$\frac{d}{d \ln \zeta} H^{\text{sub}}(x_1, x_2, b_{\perp}) = -\frac{\alpha_s C_F}{2\pi} \ln \frac{b_T^2 \mu^2}{4e^{-2\gamma_E}} H^{\text{sub}}(x_1, x_2, b_{\perp}). \quad (63)$$

This evolution equation is agree with that in [41, 42].

VI. SUMMARY

In this paper, we calculated the RG evolution equations and the rapidity scale evolution equations for four unpolarized twist-3 TMD PDFs $f^{\perp} - ig^{\perp}$, $f^{\perp} + ig^{\perp}$, h and h^{\perp} at $\mathcal{O}(\alpha_s)$. Compared to the studies in Refs. [38, 41, 42], which are based on the background field method, we derived the evolution equations straightforwardly through diagram expansion. Additionally, instead of using the δ regulator, we employed the exponential regulator to regularize the rapidity divergences.

We began by separating the correlation functions at different twists using the equation of motion. Our calculations then showed that the contributions to the evolution from the twist-2 quark-quark correlation function cancel out. As a result, the twist-3 TMD PDFs will not mix with the twist-2 TMD PDFs during the evolution process. In our calculation, we first derived the IR divergences of all relevant diagrams, where the rapidity divergences associated with the IR divergences cancel between the virtual and real corrections. We then derived the total $1/\epsilon$ divergences and rapidity divergences of these diagrams, with the rapidity divergences regularized using the exponential regulator. Finally, by subtracting the IR divergences from the sum of $1/\epsilon$ divergences and rapidity divergences, we obtained the UV divergences and the regularized rapidity divergences. Based on this, we derived the RG evolution equations and the rapidity scale evolution equations for the twist-3 TMD PDFs, which are governed by eight homogeneous equations. After performing the soft subtraction, the rapidity divergences cancel between the TMD PDFs and soft factor, leaving a dependence on ζ in the subtracted TMD PDFs. We further derived the evolution equations for the subtracted twist-3 TMD PDFs. Our evolution kernels agree with the results in Ref.[42], but differ by a sign from those in Ref.[41].

Here, we have only considered the unpolarized twist-3 TMD PDFs, but our method can

also be extended to calculate the evolution equations for polarized twist-3 TMD PDFs and TMD FFs. Additionally, given the advantages of the exponential regulator, using it could simplify the calculations for twist-3 TMD PDFs and TMD FFs. Our results can be applied to calculate twist-3 TMD PDFs at NNLO ($\mathcal{O}(\alpha_s^2)$). We leave these for future study.

VII. ACKNOWLEDGMENTS

We thank Jian-Ping Ma, Guang-Peng Zhang, Shuai Zhao and Xu-Chang Zheng for many useful discussion. We also thank S. Rodini and A. Vladimirov for discussing the results presented in their paper with us. This work is supported by the National Natural Science Foundation of China (Grant No. 12205124) and Jiangxi Provincial Natural Science Foundation (Grant No. 20242BAB20034).

Appendix A: The evolution equations in other support domains

In this appendix, we present the evolution equations in other support domains of x_i , ($i = 1, 2, 3$). The evolution equations with respect to the scale μ have following formulas

$$\frac{d}{d \ln \mu^2} H(x_1, x_2, b_\perp) = \left[\frac{\alpha_s C_F}{2\pi} \ln \frac{\mu^2}{((x_1 + x_2)P_A^+)^2} + \mathbb{K}_A \right] H(x_1, x_2, b_\perp), \quad (\text{A1})$$

for $H \in \{\tilde{f}^{\perp(1),\text{sub}} - i\tilde{g}^{\perp(1),\text{sub}}, \tilde{h}^{\text{sub}}\}$. And

$$\frac{d}{d \ln \mu^2} H(x_1, x_2, b_\perp) = \left[\frac{\alpha_s C_F}{2\pi} \ln \frac{\mu^2}{((x_1 + x_2)P_A^+)^2} + \mathbb{K}_B \right] H(x_1, x_2, b_\perp), \quad (\text{A2})$$

for $H \in \{\tilde{f}^{\perp(1),\text{sub}} + i\tilde{g}^{\perp(1),\text{sub}}, \tilde{h}^{\perp(2),\text{sub}}\}$. The evolution kernels \mathbb{K}_A and \mathbb{K}_B are depend on the domain of x_i . The results for $x_1 > 0, x_2 > 0, x_3 = x_1 + x_2 > 0$ are given in Eq. (53) and Eq. (56). The results for other domains are given as follow.

1. For $x_1 > 0, x_2 < 0, x_3 > 0$, we have

$$\begin{aligned} & \mathbb{K}_A H(x_1, x_2, b_\perp) \\ &= \frac{\alpha_s}{2\pi} \left\{ \left[\frac{3}{2} C_F + \left(C_F - \frac{C_A}{2} \right) \ln \frac{|x_1 + x_2|}{|x_1|} + \frac{C_A}{2} \ln \frac{|x_1 + x_2|}{|x_2|} + \frac{C_A}{2} i\pi \right] H(x_1, x_2, b_\perp) \right. \\ & \quad + \frac{C_A}{2} \left[\int_{-\infty}^{\infty} dy_2 \left[\theta(x_2 - y_2) \frac{x_1(x_1 + 2x_2)}{(x_1 + x_2)^2 y_1} - \theta(x_2 - y_2) \frac{x_2^2(x_1 + x_2 + y_2)}{(x_1 + x_2)^2 y_2^2} \right] H(y_1, y_2, b_\perp) \right. \\ & \quad \left. \left. + \int_{x_1}^{\infty} dy_1 \frac{x_1}{(y_1 - x_1)y_1} \left(H(y_1, y_2, b_\perp) - H(x_1, x_2, b_\perp) \right) \right] \right\} \end{aligned}$$

$$\begin{aligned}
& + \int_{-\infty}^{x_2} dy_2 \left(\frac{x_2^2}{(x_2 - y_2)y_2^2} H(y_1, y_2, b_\perp) - \frac{x_2}{(x_2 - y_2)y_2} H(x_1, x_2, b_\perp) \right) \\
& + \left(C_F - \frac{C_A}{2} \right) \int_{-\infty}^{\infty} dy_2 \left[\theta(y_2 - x_1) \frac{x_1(x_1^2 + x_1(x_2 - y_2) - 2x_2y_2)}{(x_1 + x_2)^2 y_2^2} \right. \\
& \left. + \theta(y_2 - x_1) \frac{x_2^2}{(x_1 + x_2)^2 y_1} \right] H(y_1, y_2, b_\perp) \Big\}. \tag{A3}
\end{aligned}$$

And

$$\begin{aligned}
& \mathbb{K}_B H(x_1, x_2, b_\perp) \\
& = \frac{\alpha_s}{2\pi} \left\{ \left[\frac{3}{2} C_F + \left(C_F - \frac{C_A}{2} \right) \ln \frac{|x_1 + x_2|}{|x_1|} + \frac{C_A}{2} \ln \frac{|x_1 + x_2|}{|x_2|} + \frac{C_A}{2} i\pi \right] H(x_1, x_2, b_\perp) \right. \\
& \quad + \frac{C_A}{2} \left[\int_{x_1}^{\infty} dy_1 \frac{x_1}{(y_1 - x_1)y_1} \left(H(y_1, y_2, b_\perp) - H(x_1, x_2, b_\perp) \right) \right. \\
& \quad + \int_{-\infty}^{x_2} dy_2 \left(\frac{x_2^2}{(x_2 - y_2)y_2^2} H(y_1, y_2, b_\perp) - \frac{x_2}{(x_2 - y_2)y_2} H(x_1, x_2, b_\perp) \right) \Big] \\
& \quad \left. + \left(C_F - \frac{C_A}{2} \right) \int_{-\infty}^{\infty} dy_2 \theta(y_2 - x_1) \frac{x_1}{y_2^2} H(y_1, y_2, b_\perp) \right\}. \tag{A4}
\end{aligned}$$

2. For $x_1 > 0, x_2 < 0, x_3 < 0$, we have

$$\begin{aligned}
& \mathbb{K}_A H(x_1, x_2, b_\perp) \\
& = \frac{\alpha_s}{2\pi} \left\{ \left[\frac{3}{2} C_F + \left(C_F - \frac{C_A}{2} \right) \ln \frac{|x_1 + x_2|}{|x_1|} + \frac{C_A}{2} \ln \frac{|x_1 + x_2|}{|x_2|} - \left(C_F - \frac{C_A}{2} \right) i\pi \right] H(x_1, x_2, b_\perp) \right. \\
& \quad + \frac{C_A}{2} \left[\int_{-\infty}^{\infty} dy_2 \left[\theta(x_2 - y_2) \frac{x_1(x_1 + 2x_2)}{(x_1 + x_2)^2 y_1} - \theta(x_2 - y_2) \frac{x_2^2(x_1 + x_2 + y_2)}{(x_1 + x_2)^2 y_2^2} \right] H(y_1, y_2, b_\perp) \right. \\
& \quad + \int_{x_1}^{\infty} dy_1 \frac{x_1}{(y_1 - x_1)y_1} \left(H(y_1, y_2, b_\perp) - H(x_1, x_2, b_\perp) \right) \\
& \quad + \int_{-\infty}^{x_2} dy_2 \left(\frac{x_2^2}{(x_2 - y_2)y_2^2} H(y_1, y_2, b_\perp) - \frac{x_2}{(x_2 - y_2)y_2} H(x_1, x_2, b_\perp) \right) \Big] \\
& \quad + \left(C_F - \frac{C_A}{2} \right) \int_{-\infty}^{\infty} dy_2 \left[\theta(y_2 - x_1) \frac{x_1(x_1^2 + x_1(x_2 - y_2) - 2x_2y_2)}{(x_1 + x_2)^2 y_2^2} \right. \\
& \quad \left. + \theta(y_2 - x_1) \frac{x_2^2}{(x_1 + x_2)^2 y_1} \right] H(y_1, y_2, b_\perp) \Big\}. \tag{A5}
\end{aligned}$$

And

$$\begin{aligned}
& \mathbb{K}_B H(x_1, x_2, b_\perp) \\
& = \frac{\alpha_s}{2\pi} \left\{ \left[\frac{3}{2} C_F + \left(C_F - \frac{C_A}{2} \right) \ln \frac{|x_1 + x_2|}{|x_1|} + \frac{C_A}{2} \ln \frac{|x_1 + x_2|}{|x_2|} - \left(C_F - \frac{C_A}{2} \right) i\pi \right] H(x_1, x_2, b_\perp) \right. \\
& \quad + \frac{C_A}{2} \left[\int_{x_1}^{\infty} dy_1 \frac{x_1}{(y_1 - x_1)y_1} \left(H(y_1, y_2, b_\perp) - H(x_1, x_2, b_\perp) \right) \right.
\end{aligned}$$

$$\begin{aligned}
& + \int_{-\infty}^{x_2} dy_2 \left(\frac{x_2^2}{(x_2 - y_2)y_2^2} H(y_1, y_2, b_\perp) - \frac{x_2}{(x_2 - y_2)y_2} H(x_1, x_2, b_\perp) \right) \\
& + \left(C_F - \frac{C_A}{2} \right) \int_{-\infty}^{\infty} dy_2 \theta(y_2 - x_1) \frac{x_1}{y_2^2} H(y_1, y_2, b_\perp) \Big\}. \tag{A6}
\end{aligned}$$

3. For $x_1 < 0, x_2 > 0, x_3 > 0$, we have

$$\begin{aligned}
& \mathbb{K}_A H(x_1, x_2, b_\perp) \\
& = \frac{\alpha_s}{2\pi} \left\{ \left[\frac{3}{2} C_F + \left(C_F - \frac{C_A}{2} \right) \ln \frac{|x_1 + x_2|}{|x_1|} + \frac{C_A}{2} \ln \frac{|x_1 + x_2|}{|x_2|} + \left(C_F - \frac{C_A}{2} \right) i\pi \right] H(x_1, x_2, b_\perp) \right. \\
& + \frac{C_A}{2} \left[\int_{-\infty}^{\infty} dy_2 \left[-\theta(y_2 - x_2) \frac{x_1(x_1 + 2x_2)}{(x_1 + x_2)^2 y_1} + \theta(y_2 - x_2) \frac{x_2^2(x_1 + x_2 + y_2)}{(x_1 + x_2)^2 y_2^2} \right] H(y_1, y_2, b_\perp) \right. \\
& + \int_{-\infty}^{x_1} dy_1 \frac{x_1}{(x_1 - y_1)y_1} \left(H(y_1, y_2, b_\perp) - H(x_1, x_2, b_\perp) \right) \\
& + \int_{x_2}^{\infty} dy_2 \left(\frac{x_2^2}{(y_2 - x_2)y_2^2} H(y_1, y_2, b_\perp) - \frac{x_2}{(y_2 - x_2)y_2} H(x_1, x_2, b_\perp) \right) \\
& + \left(C_F - \frac{C_A}{2} \right) \int_{-\infty}^{\infty} dy_2 \left[-\theta(x_1 - y_2) \frac{x_1(x_1^2 + x_1(x_2 - y_2) - 2x_2 y_2)}{(x_1 + x_2)^2 y_2^2} \right. \\
& \left. \left. - \theta(x_1 - y_2) \frac{x_2^2}{(x_1 + x_2)^2 y_1} \right] H(y_1, y_2, b_\perp) \right\}. \tag{A7}
\end{aligned}$$

And

$$\begin{aligned}
& \mathbb{K}_B H(x_1, x_2, b_\perp) \\
& = \frac{\alpha_s}{2\pi} \left\{ \left[\frac{3}{2} C_F + \left(C_F - \frac{C_A}{2} \right) \ln \frac{|x_1 + x_2|}{|x_1|} + \frac{C_A}{2} \ln \frac{|x_1 + x_2|}{|x_2|} + \left(C_F - \frac{C_A}{2} \right) i\pi \right] H(x_1, x_2, b_\perp) \right. \\
& + \frac{C_A}{2} \left[\int_{-\infty}^{x_1} dy_1 \frac{x_1}{(x_1 - y_1)y_1} \left(H(y_1, y_2, b_\perp) - H(x_1, x_2, b_\perp) \right) \right. \\
& + \int_{x_2}^{\infty} dy_2 \left(\frac{x_2^2}{(y_2 - x_2)y_2^2} H(y_1, y_2, b_\perp) - \frac{x_2}{(y_2 - x_2)y_2} H(x_1, x_2, b_\perp) \right) \\
& \left. \left. - \left(C_F - \frac{C_A}{2} \right) \int_{-\infty}^{\infty} dy_2 \theta(x_1 - y_2) \frac{x_1}{y_2^2} H(y_1, y_2, b_\perp) \right] \right\}. \tag{A8}
\end{aligned}$$

4. For $x_1 < 0, x_2 > 0, x_3 < 0$, we have

$$\begin{aligned}
& \mathbb{K}_A H(x_1, x_2, b_\perp) \\
& = \frac{\alpha_s}{2\pi} \left\{ \left[\frac{3}{2} C_F + \left(C_F - \frac{C_A}{2} \right) \ln \frac{|x_1 + x_2|}{|x_1|} + \frac{C_A}{2} \ln \frac{|x_1 + x_2|}{|x_2|} - \frac{C_A}{2} i\pi \right] H(x_1, x_2, b_\perp) \right. \\
& + \frac{C_A}{2} \left[\int_{-\infty}^{\infty} dy_2 \left[-\theta(y_2 - x_2) \frac{x_1(x_1 + 2x_2)}{(x_1 + x_2)^2 y_1} + \theta(y_2 - x_2) \frac{x_2^2(x_1 + x_2 + y_2)}{(x_1 + x_2)^2 y_2^2} \right] H(y_1, y_2, b_\perp) \right. \\
& + \int_{-\infty}^{x_1} dy_1 \frac{x_1}{(x_1 - y_1)y_1} \left(H(y_1, y_2, b_\perp) - H(x_1, x_2, b_\perp) \right) \\
& \left. \left. \right] \right\}
\end{aligned}$$

$$\begin{aligned}
& + \int_{x_2}^{\infty} dy_2 \left(\frac{x_2^2}{(y_2 - x_2)y_2^2} H(y_1, y_2, b_{\perp}) - \frac{x_2}{(y_2 - x_2)y_2} H(x_1, x_2, b_{\perp}) \right) \\
& + \left(C_F - \frac{C_A}{2} \right) \int_{-\infty}^{\infty} dy_2 \left[-\theta(x_1 - y_2) \frac{x_1(x_1^2 + x_1(x_2 - y_2) - 2x_2y_2)}{(x_1 + x_2)^2 y_2^2} \right. \\
& \left. - \theta(x_1 - y_2) \frac{x_2^2}{(x_1 + x_2)^2 y_1} \right] H(y_1, y_2, b_{\perp}) \Big\}. \tag{A9}
\end{aligned}$$

And

$$\begin{aligned}
& \mathbb{K}_B H(x_1, x_2, b_{\perp}) \\
& = \frac{\alpha_s}{2\pi} \left\{ \left[\frac{3}{2} C_F + \left(C_F - \frac{C_A}{2} \right) \ln \frac{|x_1 + x_2|}{|x_1|} + \frac{C_A}{2} \ln \frac{|x_1 + x_2|}{|x_2|} - \frac{C_A}{2} i\pi \right] H(x_1, x_2, b_{\perp}) \right. \\
& \quad + \frac{C_A}{2} \left[\int_{-\infty}^{x_1} dy_1 \frac{x_1}{(x_1 - y_1)y_1} \left(H(y_1, y_2, b_{\perp}) - H(x_1, x_2, b_{\perp}) \right) \right. \\
& \quad + \int_{x_2}^{\infty} dy_2 \left(\frac{x_2^2}{(y_2 - x_2)y_2^2} H(y_1, y_2, b_{\perp}) - \frac{x_2}{(y_2 - x_2)y_2} H(x_1, x_2, b_{\perp}) \right) \Big] \\
& \quad \left. - \left(C_F - \frac{C_A}{2} \right) \int_{-\infty}^{\infty} dy_2 \theta(x_1 - y_2) \frac{x_1}{y_2^2} H(y_1, y_2, b_{\perp}) \right\}. \tag{A10}
\end{aligned}$$

5. For $x_1 < 0, x_2 < 0, x_3 < 0$, we have

$$\begin{aligned}
& \mathbb{K}_A H(x_1, x_2, b_{\perp}) \\
& = \frac{\alpha_s}{2\pi} \left\{ \left[\frac{3}{2} C_F + \left(C_F - \frac{C_A}{2} \right) \ln \frac{|x_1 + x_2|}{|x_1|} + \frac{C_A}{2} \ln \frac{|x_1 + x_2|}{|x_2|} \right] H(x_1, x_2, b_{\perp}) \right. \\
& \quad + \frac{C_A}{2} \left[\int_{-\infty}^{\infty} dy_2 \left[-\theta(y_2 - x_2) \frac{x_1(x_1 + 2x_2)}{(x_1 + x_2)^2 y_1} - \theta(x_2 - y_2) \frac{x_2^2(x_1 + x_2 + y_2)}{(x_1 + x_2)^2 y_2^2} \right] H(y_1, y_2, b_{\perp}) \right. \\
& \quad + \int_{-\infty}^{x_1} dy_1 \frac{x_1}{(x_1 - y_1)y_1} \left(H(y_1, y_2, b_{\perp}) - H(x_1, x_2, b_{\perp}) \right) \\
& \quad + \int_{-\infty}^{x_2} dy_2 \left(\frac{x_2^2}{(x_2 - y_2)y_2^2} H(y_1, y_2, b_{\perp}) - \frac{x_2}{(x_2 - y_2)y_2} H(x_1, x_2, b_{\perp}) \right) \Big] \\
& \quad + \left(C_F - \frac{C_A}{2} \right) \int_{-\infty}^{\infty} dy_2 \left[-\theta(x_1 - y_2) \frac{x_1(x_1^2 + x_1(x_2 - y_2) - 2x_2y_2)}{(x_1 + x_2)^2 y_2^2} \right. \\
& \quad \left. + \theta(y_2 - x_1) \frac{x_2^2}{(x_1 + x_2)^2 y_1} \right] H(y_1, y_2, b_{\perp}) \Big\}. \tag{A11}
\end{aligned}$$

And

$$\begin{aligned}
& \mathbb{K}_B H(x_1, x_2, b_{\perp}) \\
& = \frac{\alpha_s}{2\pi} \left\{ \left[\frac{3}{2} C_F + \left(C_F - \frac{C_A}{2} \right) \ln \frac{|x_1 + x_2|}{|x_1|} + \frac{C_A}{2} \ln \frac{|x_1 + x_2|}{|x_2|} \right] H(x_1, x_2, b_{\perp}) \right. \\
& \quad + \frac{C_A}{2} \left[\int_{-\infty}^{x_1} dy_1 \frac{x_1}{(x_1 - y_1)y_1} \left(H(y_1, y_2, b_{\perp}) - H(x_1, x_2, b_{\perp}) \right) \right.
\end{aligned}$$

$$\begin{aligned}
& + \int_{-\infty}^{x_2} dy_2 \left(\frac{x_2^2}{(x_2 - y_2)y_2^2} H(y_1, y_2, b_\perp) - \frac{x_2}{(x_2 - y_2)y_2} H(x_1, x_2, b_\perp) \right) \\
& - \left(C_F - \frac{C_A}{2} \right) \int_{-\infty}^{\infty} dy_2 \theta(x_1 - y_2) \frac{x_1}{y_2^2} H(y_1, y_2, b_\perp) \Big\}. \tag{A12}
\end{aligned}$$

Finally, the evolution equations with respect to the scale ζ are same for all domains, which read

$$\frac{d}{d \ln \zeta} H(x_1, x_2, b_\perp) = - \frac{\alpha_s C_F}{2\pi} \ln \frac{b_T^2 \mu^2}{4e^{-2\gamma_E}} H(x_1, x_2, b_\perp), \tag{A13}$$

for $H \in \{\tilde{f}^{\perp(1),\text{sub}} - i\tilde{g}^{\perp(1),\text{sub}}, \tilde{f}^{\perp(1),\text{sub}} + i\tilde{g}^{\perp(1),\text{sub}}, \tilde{h}^{\text{sub}}, \tilde{h}^{\perp(2),\text{sub}}\}$.

-
- [1] X.-d. Ji, J.-p. Ma, and F. Yuan, *QCD factorization for semi-inclusive deep-inelastic scattering at low transverse momentum*, *Phys. Rev. D* **71** (2005) 034005 [[hep-ph/0404183](#)].
 - [2] X.-d. Ji, J.-P. Ma, and F. Yuan, *QCD factorization for spin-dependent cross sections in DIS and Drell-Yan processes at low transverse momentum*, *Phys. Lett. B* **597** (2004) 299–308 [[hep-ph/0405085](#)].
 - [3] J. C. Collins and A. Metz, *Universality of soft and collinear factors in hard-scattering factorization*, *Phys. Rev. Lett.* **93** (2004) 252001 [[hep-ph/0408249](#)].
 - [4] J. C. Collins, D. E. Soper, and G. F. Sterman, *Transverse Momentum Distribution in Drell-Yan Pair and W and Z Boson Production*, *Nucl. Phys. B* **250** (1985) 199–224.
 - [5] J. Collins, *Foundations of Perturbative QCD*, Camb. Monogr. Part. Phys. Nucl. Phys. Cosmol. **32**, 1-624 (2011) Cambridge University Press, 2023.
 - [6] J. C. Collins and D. E. Soper, *Parton Distribution and Decay Functions*, *Nucl. Phys.* **B194** (1982) 445 [[INSPIRE](#)].
 - [7] T. Becher and M. Neubert, *Drell-Yan Production at Small q_T , Transverse Parton Distributions and the Collinear Anomaly*, *Eur. Phys. J. C* **71** (2011) 1665 [[arXiv:1007.4005](#)].
 - [8] T. Becher and G. Bell, *Analytic Regularization in Soft-Collinear Effective Theory*, *Phys. Lett. B* **713** (2012) 41–46 [[arXiv:1112.3907](#)].
 - [9] J.-y. Chiu, A. Jain, D. Neill, and I. Z. Rothstein, *The Rapidity Renormalization Group*, *Phys. Rev. Lett.* **108** (2012) 151601 [[arXiv:1104.0881](#)].

- [10] J.-Y. Chiu, A. Jain, D. Neill, and I. Z. Rothstein, *A Formalism for the Systematic Treatment of Rapidity Logarithms in Quantum Field Theory*, *JHEP* **05** (2012) 084 [[arXiv:1202.0814](#)].
- [11] M. G. Echevarria, A. Idilbi, and I. Scimemi, *Factorization Theorem For Drell-Yan At Low q_T And Transverse Momentum Distributions On-The-Light-Cone*, *JHEP* **07** (2012) 002 [[arXiv:1111.4996](#)].
- [12] M. G. Echevarria, A. Idilbi, and I. Scimemi, *Soft and Collinear Factorization and Transverse Momentum Dependent Parton Distribution Functions*, *Phys. Lett. B* **726** (2013) 795–801 [[arXiv:1211.1947](#)].
- [13] Z.-F. Deng, W. Wang, and J. Zeng, *Transverse-momentum-dependent wave functions and soft functions at one-loop in large momentum effective theory*, *JHEP* **09** (2022) 046 [[arXiv:2207.07280](#)].
- [14] Y. Li, D. Neill, and H. X. Zhu, *An exponential regulator for rapidity divergences*, *Nucl. Phys. B* **960** (2020) 115193 [[arXiv:1604.00392](#)].
- [15] R. Boussarie *et al.*, *TMD Handbook*, [[arXiv:2304.03302](#)].
- [16] M. A. Ebert, I. W. Stewart, and Y. Zhao, *Towards Quasi-Transverse Momentum Dependent PDFs Computable on the Lattice*, *JHEP* **09** (2019) 037 [[arXiv:1901.03685](#)].
- [17] T. Gehrmann, T. Lubbert, and L. L. Yang, *Transverse parton distribution functions at next-to-next-to-leading order: the quark-to-quark case*, *Phys. Rev. Lett.* **109** (2012) 242003 [[arXiv:1209.0682](#)].
- [18] T. Gehrmann, T. Luebbert, and L. L. Yang, *Calculation of the transverse parton distribution functions at next-to-next-to-leading order*, *JHEP* **06** (2014) 155 [[arXiv:1403.6451](#)].
- [19] M. G. Echevarria, I. Scimemi, and A. Vladimirov, *Unpolarized Transverse Momentum Dependent Parton Distribution and Fragmentation Functions at next-to-next-to-leading order*, *JHEP* **09** (2016) 004 [[arXiv:1604.07869](#)].
- [20] M.-X. Luo, X. Wang, X. Xu, L. L. Yang, T.-Z. Yang, and H. X. Zhu, *Transverse Parton Distribution and Fragmentation Functions at NNLO: the Quark Case*, *JHEP* **10** (2019) 083 [[arXiv:1908.03831](#)].
- [21] M.-X. Luo, T.-Z. Yang, H. X. Zhu, and Y. J. Zhu, *Transverse Parton Distribution and Fragmentation Functions at NNLO: the Gluon Case*, *JHEP* **01** (2020) 040 [[arXiv:1909.13820](#)].
- [22] M.-x. Luo, T.-Z. Yang, H. X. Zhu, and Y. J. Zhu, *Quark Transverse Parton Distribution at*

- the Next-to-Next-to-Next-to-Leading Order*, *Phys. Rev. Lett.* **124** (2020) 092001 [arXiv:1912.05778].
- [23] M.-x. Luo, T.-Z. Yang, H. X. Zhu, and Y. J. Zhu, *Unpolarized quark and gluon TMD PDFs and FFs at N^3LO* , *JHEP* **06** (2021) 115 [arXiv:2012.03256].
- [24] M. A. Ebert, B. Mistlberger, and G. Vita, *Transverse momentum dependent PDFs at N^3LO* , *JHEP* **09** (2020) 146 [arXiv:2006.05329].
- [25] M. A. Ebert, B. Mistlberger, and G. Vita, *TMD fragmentation functions at N^3LO* , *JHEP* **07** (2021) 121 [arXiv:2012.07853].
- [26] T. Gehrmann, E. W. N. Glover, T. Huber, N. Ikizlerli, and C. Studerus, *Calculation of the quark and gluon form factors to three loops in QCD*, *JHEP* **06** (2010) 094 [arXiv:1004.3653].
- [27] A. Vladimirov, *Structure of rapidity divergences in multi-parton scattering soft factors*, *JHEP* **04** (2018) 045 [arXiv:1707.07606].
- [28] Y. Li and H. X. Zhu, *Bootstrapping Rapidity Anomalous Dimensions for Transverse-Momentum Resummation*, *Phys. Rev. Lett.* **118** (2017) 022004 [arXiv:1604.01404].
- [29] P. J. Mulders and R. D. Tangerman, *The Complete tree level result up to order $1/Q$ for polarized deep inelastic leptonproduction*, *Nucl. Phys. B* **461** (1996) 197–237 [hep-ph/9510301]. [Erratum: Nucl.Phys.B 484, 538–540 (1997)].
- [30] D. Boer, P. J. Mulders, and F. Pijlman, *Universality of T odd effects in single spin and azimuthal asymmetries*, *Nucl. Phys. B* **667** (2003) 201–241 [hep-ph/0303034].
- [31] A. Bacchetta, P. J. Mulders, and F. Pijlman, *New observables in longitudinal single-spin asymmetries in semi-inclusive DIS*, *Phys. Lett. B* **595** (2004) 309–317 [hep-ph/0405154].
- [32] A. Bacchetta, M. Diehl, K. Goeke, A. Metz, P. J. Mulders, and M. Schlegel, *Semi-inclusive deep inelastic scattering at small transverse momentum*, *JHEP* **02** (2007) 093 [hep-ph/0611265].
- [33] D. Boer, R. Jakob, and P. J. Mulders, *Asymmetries in polarized hadron production in e^+e^- annihilation up to order $1/Q$* , *Nucl. Phys. B* **504** (1997) 345–380 [hep-ph/9702281].
- [34] Z. Lu and I. Schmidt, *Transverse momentum dependent twist-three result for polarized Drell-Yan processes*, *Phys. Rev. D* **84** (2011) 114004 [arXiv:1109.3232].
- [35] A. Bacchetta, D. Boer, M. Diehl, and P. J. Mulders, *Matches and mismatches in the*

- descriptions of semi-inclusive processes at low and high transverse momentum, *JHEP* **08** (2008) 023 [[arXiv:0803.0227](#)].
- [36] A. P. Chen and J. P. Ma, *Light-Cone Singularities and Transverse-Momentum-Dependent Factorization at Twist-3*, *Phys. Lett. B* **768** (2017) 380–386 [[arXiv:1610.08634](#)].
 - [37] A. Bacchetta, G. Bozzi, M. G. Echevarria, C. Pisano, A. Prokudin, and M. Radici, *Azimuthal asymmetries in unpolarized SIDIS and Drell-Yan processes: a case study towards TMD factorization at subleading twist*, *Phys. Lett. B* **797** (2019) 134850 [[arXiv:1906.07037](#)].
 - [38] A. Vladimirov, V. Moos, and I. Scimemi, *Transverse momentum dependent operator expansion at next-to-leading power*, *JHEP* **01** (2022) 110 [[arXiv:2109.09771](#)].
 - [39] M. A. Ebert, A. Gao, and I. W. Stewart, *Factorization for azimuthal asymmetries in SIDIS at next-to-leading power*, *JHEP* **06** (2022) 007 [[arXiv:2112.07680](#)]. [Erratum: *JHEP* 07, 096 (2023)].
 - [40] L. Gamberg, Z.-B. Kang, D. Y. Shao, J. Terry, and F. Zhao, *Transverse-momentum-dependent factorization at next-to-leading power*, [[arXiv:2211.13209](#)].
 - [41] S. Rodini and A. Vladimirov, *Definition and evolution of transverse momentum dependent distribution of twist-three*, *JHEP* **08** (2022) 031 [[arXiv:2204.03856](#)]. [Erratum: *JHEP* 12, 048 (2022)].
 - [42] S. Rodini and A. Vladimirov, *Transverse momentum dependent factorization for SIDIS at next-to-leading power*, [[arXiv:2306.09495](#)].
 - [43] X.-d. Ji and F. Yuan, *Parton distributions in light cone gauge: Where are the final state interactions?*, *Phys. Lett. B* **543** (2002) 66–72 [[hep-ph/0206057](#)].
 - [44] A. V. Belitsky, X. Ji, and F. Yuan, *Final state interactions and gauge invariant parton distributions*, *Nucl. Phys. B* **656** (2003) 165–198 [[hep-ph/0208038](#)].
 - [45] I. O. Cherednikov and N. G. Stefanis, *Renormalization, Wilson lines, and transverse-momentum dependent parton distribution functions*, *Phys. Rev. D* **77** (2008) 094001 [[arXiv:0710.1955](#)].
 - [46] A. Idilbi and I. Scimemi, *Singular and Regular Gauges in Soft Collinear Effective Theory: The Introduction of the New Wilson Line T* , *Phys. Lett. B* **695** (2011) 463–468 [[arXiv:1009.2776](#)].
 - [47] D. Boer, L. Gamberg, B. Musch, and A. Prokudin, *Bessel-Weighted Asymmetries in Semi*

- Inclusive Deep Inelastic Scattering*, *JHEP* **10** (2011) 021 [[arXiv:1107.5294](#)].
- [48] J. P. Ma and G. P. Zhang, *Evolution of Chirality-odd Twist-3 Fragmentation Functions*, *Phys. Lett. B* **772** (2017) 559–566 [[arXiv:1701.04141](#)].
- [49] A. V. Manohar and I. W. Stewart, *The Zero-Bin and Mode Factorization in Quantum Field Theory*, *Phys. Rev. D* **76** (2007) 074002 [[hep-ph/0605001](#)].